Detailed Analysis of Residual Volatiles in Chars from the Pyrolysis of Biomass and Lignite

Detailed Analysis of Residual Volatiles in Chars from the Pyrolysis of Biomass and Lignite

Hua Yang,[†] Shinji Kudo,[‡] Seira Hazeyama,[§] Koyo Norinaga,[§] Ondřej Mašek[||] and Jun-ichiro Hayashi[†,‡,§,]*

[†] Interdisciplinary Graduate School of Engineering Sciences, Kyushu University, 6-1, Kasuga Koen, Kasuga 816-8580, Japan

[‡]Center for Education and Research of Carbon Resources, Kyushu University, 6-1, Kasuga Koen, Kasuga 816-8580, Japan

[§] Institute for Materials Chemistry and Engineering, Kyushu University, 6-1, Kasuga Koen, Kasuga 816-8580, Japan

[||] UK Biochar Research Centre, University of Edinburgh, Edinburgh EH9 3JN, UK

ABSTRACT: Pyrolysis of biomass or coal, if operated at temperature high enough to complete tar evolution, is expected to give resulting char a tar-free nature. Use of such tar-free char instead of the original fuel in gasification would reduce or even completely eliminate the need for use of complex devices/mechanisms for tar/soot removal. Increasing pyrolysis temperature may not only decrease content of residual tar in the char, but also reduce its reactivity in the gasification. There is thus a range of optimum pyrolysis temperatures depending on the original fuel and type/mode of gasification, which

yields char of suitable quality. In this work, a variety of char samples were prepared by pyrolysis (first pyrolysis) of three different woody biomass feedstock and a Victorian lignite with heating rate and peak temperature of 10 °C/min and 450–750 °C, respectively, and were further subjected to flash pyrolysis (second pyrolysis) at 920 °C. A gas-chromatography mass-spectrometry (GC/MS) detected more than 200 compounds in the volatile products from the second pyrolysis, and quantified 58 aromatic compounds over a range from benzene to coronene, which accounted for more than 85% of the compounds detected based on peak area on the total ion chromatogram. Total emission of tar, defined as the aromatics except mono-aromatic hydrocarbons, from the biomass chars was 0.03–0.08 wt%-char even at the first pyrolysis temperature of 450 °C, and further decreased to a level around 0.01 wt% by raising the temperature to 600 °C. It was also found that despite containing as much as 20–27 wt% of residual volatile matter, chars produced by pyrolysis at 500 °C contained less than 0.1 wt% of residual tar.

1. INTRODUCTION

Char from the pyrolysis of biomass, which is often termed biochar, is a solid fuel with higher calorific value and grindability than the original one[1], an adsorbent with high adsorption ability, a reducing agent for metallurgy or foundry, or a carbon-rich agricultural material for improving quality of soil and carbon sequestration.[2-4] Biochar is a solid byproduct from biomass pyrolysis with a main purpose to produce bio-oil, and therefore, its effective utilization enhances the feasibility of the pyrolysis. The biochar is often more important in terms of chemical energy than the bio-oil when the pyrolysis is designed to increase or maximize the biochar yield.[5,6].

This work is focused on production of biochar with a tar-free (smokeless) nature by pyrolyzing biomass until complete evolution of tar and tar precursors (bio-oil) evolution. There have been a number of studies on biomass gasification for syngas production and power generation, and removal of tar has

been identified as a most important challenge to successful implementation of this technology.[7,8] A lot of research and development has been focused on elimination of tar inside the gasifier employing non-catalytic reforming at elevated temperature[9] or catalytic reforming at lower temperature.[10-12] However, despite considerable progress achieved, tar-related problems such as substantial loss of chemical energy, incomplete tar removal and catalyst deactivation still remain a challenge to technical/economic feasibility of biomass gasification.

Gasification of "tar-free" biochar instead of parent biomass will enable production of clean gas without any processes for tar elimination, which would provide significant benefits over existing solutions. An advanced integrated gasification fuel cell (IGFC) system has recently been proposed with a theoretical electrical efficiency of 89%, utilizing a steam turbine but without a gas turbine.[13] In this IGFC, heat generated by the solid oxide fuel cells (SOFCs) is directly transferred to drive steam gasification of a solid fuel in a fluidized bed and is recuperated into chemical energy of H_2 as the fuel for the SOFCs. The fluidized bed gasification will be operated at temperature well below 900 °C to achieve high thermodynamic efficiency, but at the same time needed to be able to produce clean gas suitable for the SOFCs with minimized purification of the fuel gas. Use of tar-free biochar, in particular, that from woody biomass with low contents of ash and trace elements, is a most reasonable option for tar-free steam gasification of biomass. Victorian lignite has properties similar to those of biomass such as high oxygen content and low ash content.[14] The lignite char can potentially be an excellent fuel for the steam gasification. It is reported that the steam gasification of lignite char is greatly inhibited by the presence of pyrolysis-derived volatiles that are formed by the pyrolysis simultaneously with the char, in particular, tar and hydrocarbon gases, as well as H_2.[14] Elimination of these species prior to the char gasification thus has an advantage over the gasification of the parent fuel. Although not reported so far, such inhibition of the char gasification, would also occur in the biomass gasification.

In addition, due to gasification temperature required in an IGFC, as low as 800 °C or even lower, it is necessary to ensure high reactivity of the tar-free biochar in the gasification. During the gasification of biochar, syngas is formed by not only the steam gasification of the char but also its thermal cracking.[15,16] Light gases such as H_2, CO, CO_2 and CH_4 from the thermal cracking contribute to a portion of the syngas. More importantly, simultaneous progress of the thermal cracking and steam gasification, which is possible under rapid heating of the char, formation of active sites by the thermal cracking greatly contributes to enhancement of the gasification.[15,16] The extent of such thermal cracking is a function of temperature for char preparation. In other words, lower pyrolysis temperature is preferred to preserve more precursors of light gases. Pyrolyzing the biomass at temperature higher than that for the gasification is an idea to completely avoid the tar emission during the gasification, but it may lose the reactivity of resulting biochar toward the thermal cracking and also toward the steam gasification. Biochar could also be applied to advanced power generation systems with direct carbon fuel cells (DCFCs).[17,18] For biochar to be suitable for use in DCFC power generation, it needs to have a sufficiently high reactivity with molten carbonate or metal oxide as well as properties such as minimized contents of impurities. Therefore, there seems to be an optimum range of pyrolysis temperatures suitable for production of tar-free, yet sufficiently reactive biochar.

The range of acceptable tar concentration in the syngas or fuel gas depends on its end use, such as power generator or chemical process. When the gasification of biomass with air/steam or oxygen/steam is combined with power generation with internal combustion engines, it is normally recommended that the tar concentration in the fuel gas is lower than 10^2 mg Nm^{-3} on a dry basis,[7] and this corresponds to a tar yield of around 10^{-2} wt%-dry-biomass. In the case of fuel cells, upper limit of the tar concentration is even lower.[7] The residual tar content in biochar, if it is to be gasified without the need for either an in-reactor or downstream tar elimination, hence needs to be below the above-mentioned level.

It is believed for biomass pyrolysis that the tar evolution is fully or nearly completed at 500–600 °C.[19] It is, however, difficult or impossible to guarantee tar-free nature of a biochar even if it has been produced by pyrolysis at such temperature. Moreover, there has been no scientific definition of degree of tar-freeness. Very recently, solvent-extractable material in biochar was investigated, and polyaromatic hydrocarbons (PAHs) were quantified.[20,21] However, the amount and composition of such PAHs are not necessarily direct measures for tar release from the biochar at elevated temperature. This paper proposes a way to quantify emission of aromatic compounds from char upon heating to temperature relevant to gasification, even when their total emission is as low as 10^{-4} wt%, and reports characteristics of emission of aromatic compounds during heating of char, prepared by pyrolysis of different types of woody biomass and a Victorian lignite at 450–750 °C.

2. EXPERIMENTAL

2.1. Material. Pine (cryptomeria japonica), cedar (cryptomeria japonica) and mallee (eucalyptus) and a Victorian lignite (Loy Yang) were employed as the starting samples. Their particle sizes were in a range from 125 to 500 μm. These samples were dried prior to use by heating in atmospheric flow of nitrogen at 110 °C for 1 h. Aromatic compounds of reagent grades were purchased and used as the standard compounds for quantitative pyrolysis-gas chromatography/mass spectrometry (Pyrolysis-GC/MS).

2.2. Pyrolysis for Char Preparation. The starting biomass and lignite samples were subjected to slow pyrolysis in a horizontal reactor that was made of a transparent quartz tube with inner diameter of 25 mm. This pyrolysis is hereafter referred to as the first pyrolysis. A thin bed of a 0.1 g of the sample was placed in a quartz boat, which was then inserted into the reactor. The sample was heated to a prescribed peak temperature ($T_{py,1}$ = 450, 500, 550, 600, 650, 700 or 750 °C) at a heating rate of 10 °C/min, and immediately after reaching the desired temperature, cooled to ambient temperature at an

initial rate of 50–100 °C/min. An atmospheric and continuous flow of nitrogen (purity > 99.99995 vol%) was used through the heating/cooling period to avoid diffusion of volatiles back to the pyrolyzing solid. A condensation train of an aerosol filter, a condenser (at −70 °C) and a gasbag was installed in the reactor downstream. Non-condensable gases (H_2, CO, CO_2, CH_4, C_2H_4 and C_2H_6) were quantified by gas chromatography. A gas chromatograph (GC) equipped with a thermal conductivity detector (Shimadzu, GC-8A) was employed for the gas analysis. The char prepared by the first pyrolysis with peak temperature of $T_{py,1}$ °C will be denoted by char-1-$T_{py,1}$, or otherwise, just by char-1 if no need of specifying $T_{py,1}$. The elemental compositions of the char-1 samples are presented in Table 1 as their elemental compositions together with those of the parent feedstock. For the pyrolysis with $T_{py,1}$ of 600 °C, the yield of water, which was collected in the condenser, was measured by Karl Fischer Titrimetry.

2.3. Pyrolysis-GC of Char from First Pyrolysis. Pyrolysis-GC of the char-1 samples was carried out with a commercially available pyrolyzer (Japan Analytical Industry Co., Ltd., Curie-Point Pyrolyzer, JHP-22), which was connected to the same GC as used for analyzing gases from the first pyrolysis. About 1 mg of the dried char-1 was wrapped with a ferromagnetic foil (Japan Analytical Industry Co., Ltd., F920) of that Curie-point temperature was 920 °C, and charged into a quartz tube reactor, which was then placed in the pyrolyzer. The char-1 was heated inductively up to the Curie-point temperature of the foil, *i.e.*, 920 °C, at a heating rate of around 3000 °C/s (guaranteed by constructor), and held for 10 s at the temperature. Selective heating of the ferromagnetic foil and solid sample was a particular feature of the Curie-point pyrolyzer, which enabled to minimize the gas-phase reactions of the volatiles. During the heating, there was continuous flow of helium or nitrogen through the quartz tube so that the entire portion of the gaseous products were sent to the GC and injected into the analytical column. The pyrolysis of char-1 in this way and the produced char will be referred to as the second pyrolysis and char-2, respectively. Light gases such as H_2, CO, CO_2, H_2O, CH_4, C_2H_4, and C_2H_6, and water vapor were detected and quantified. The nitrogen and helium carriers were employed for analyzing H_2

and the other gases and water vapor, respectively. More details of the pyrolysis-GC were reported elsewhere.[22]

2.4. Pyrolysis-GC/MS of Char from First Pyrolysis. The second pyrolysis with the same peak temperature and holding time as mentioned above was performed with another portable pyrolyzer (Japan Analytical Industry Co., Ltd., Curie-Point Injector JCI-22). The pyrolyzer was connected to a Perkin-Elmer Clarus 600C gas chromatography/mass-spectrometry (GC/MS). The GC was equipped with a capillary column; a TC-1701 (GL Science Inc., 60 m, 0.25 mm inner diameter, and 0.25 μm film thickness) or an InertCap® 1 (GL Science Inc., 60 m, 0.25 mm inner diameter, and 0.25 μm film thickness). The mass spectrometer was configured for electron impact ionization at 70 eV. The interface and source temperatures were both 250 °C. The pyrolysis-derived volatiles were directly injected into the GC/MS through its injector at 345 °C together with helium (purity > 99.9999 vol%) on a splitless mode or with a split ratio of 5 or 18. The capillary column was heated according to the following temperature program: holding at 40 °C for 5 min, heating to 250 °C at 4 °C/min, holding at 250 °C for 20 min (in case of TC-1701) or holding at 40 °C for 5 min, heating to 325 °C at 4 °C/min, holding at 325 °C for 20 min (InertCap® 1). Chromatograms were recorded on a full scan mode (m/z range of 50–350) and a selected ion recording (SIR) mode simultaneously. The former mode was mainly for identification of volatile compounds, while the latter for quantification of selected compounds.

Among the volatile products detected by the GC/MS, 58 aromatic compounds were quantified. Table 2 lists the compounds that were detected by the GC/MS for the pyrolysis of the char-1-450 and char-1-600 from the pine. This table also indicates the quantified compounds except 1-naphthol and 1,2-benzenediol (catechol), which were not confirmed in total ion chromatograms in a full scan mode but detected/quantified in an SIR mode. As seen in the table, the total numbers of the detected compounds were 178 and 93 for the pyrolysis of char-1-450 and char-1-600, respectively. Regardless of the combination of the starting sample and $T_{py,1}$, the number of quantified compounds, 58, was smaller than

that of the detected compounds, which was often more than 100. Table 2 also reports peak areas of the individual compounds (after normalization by the area of peak assigned to benzene), which were determined from total ion chromatograms, showing that the total peak area of the quantified compounds accounts for around 90% or even more of that of the detected compounds. It was thus believed that the quantified 58 compounds accounted for a major portion of the aromatic compounds released from the char-1. Such sufficiently large peak-area-based fraction of the detected compounds was confirmed for the pyrolysis of the other char-1 samples. Non-aromatic C_4-C_6 compounds, methylfurans and cyclopentadienes were also detected, and are listed in Table 3. These compounds were not regarded as components of tar, and therefore not quantified. The total peak area of the compounds given in Table 3 was 5–6% of that given in Table 2.

Quantification of the 58 aromatic compounds was based on not a total ion chromatogram but chromatograms specific to their molecular masses (exactly saying, masses of parent ions), which were obtained in the SIR mode. Figure 1 shows examples of chromatograms specific to m/z = 300, which was recorded for quantification of coronene, compounds with the largest molecular mass among those detected. Its average yield was as low as $8 \cdot 10^{-8}$ wt% (amount; 0.8 pg) of the char-1-550 from the lignite, but was reproducible as seen in the figure. Yields of the individual compounds were determined by averaging those from independent 2–5 pyrolysis-GC/MS runs. Table 4 presents reproducibility of the yields for 9 aromatic compounds from the second pyrolysis, as examples. For every set of the char sample and quantified compounds, the minimum and maximum yields among those taken in determining the average yield are compared in the table. Thus, a value close to unity means better reproducibility. The ratios are in a range of 0.5–1.0, but mainly in that of 0.7–1.0. The results showed that reproducibility for compounds with higher yields was better than for those with lower yields.

2.5. Definition of Tar. In the present paper, tar is defined as the quantified aromatic compounds except for mono-aromatic hydrocarbons (*i.e.*, benzene, toluene, xylenes, ethylbenzene and styrene = BTXES). None of the C_4-C_6 compounds listed in Table 3 were involved in the tar, as stated earlier.

3. RESULTS AND DISCUSSION

3.1. General Characteristics of First and Second Pyrolysis. Figure 2 shows the effects of $T_{py,1}$ on the yields of char-1 and liquid that consisted of the condensable organic matter and water. The individual char-1 yields decrease gradually with $T_{py,1}$. This trend common among the four different fuels suggests that $T_{py,1}$ higher than 450 °C or 500 °C is high enough to complete evolution of the major portion of tar from the pyrolyzing biomass and lignite, respectively. In fact, the liquid yields seem to approach maximum yields. The yields of water for the pyrolysis of the cedar, mallee, pine and lignite at $T_{py,1}$ = 600 °C were 18–23, 18–23, 15–19 and 10–14 wt%-dry, respectively. Assuming that mean yield of organic liquid can be calculated by subtracting the total liquid yield by the water yield, the mean organic liquid yields were 43, 37, 46 and 13 wt% for the cedar, mallee, pine and lignite, respectively.

Figure 3 shows a result from the second pyrolysis of char-1. In this figure, the total yield of non-condensable gas and water is compared with the total volatile matter yield, which was determined from the difference in the mass between the char-1 and char-2. It is seen that these yields are in good agreement with each other within a certain degree of error for the individual combinations of $T_{py,1}$ and starting fuel. This result means that the emission of tar from char-1, if any, was insignificant, and it is also consistent with the results shown in Figure 2.

The flash pyrolysis was also performed for the starting fuel at 920 °C, although results are not shown in this paper. A major part of tar was condensed on the inner wall of the quartz reactor tube as brown colored solid/liquid material. On the other hand, in the case of pyrolysis of the char-1 samples, no condensation of such matter was detected. Figure 3 also demonstrates that the total volatile matter yield

ranged from 10 wt% (lignite char-1-650) to 32 wt% (mallee char-1-450), and many of the char-1 samples evolved more than 20 wt% of volatiles. Thus, the char-1 samples contained substantial amounts of volatiles but very little tar.

The effect of $T_{py,1}$ on the net yield of char-2, *i.e.*, its yield on the basis of mass of the starting fuel, is shown in Figure 4. $T_{py,1}$ hardly influenced the net char yield. The net char-2 yield was thus determined by the temperature for the second pyrolysis within the range of $T_{py,1}$ examined in the present study. It was suggested that the char-2 samples for different $T_{py,1}$ had nearly the same or very similar properties. The effect of $T_{py,1}$ on the evolution of light gases during the second pyrolysis was investigated. Figure 5 plots the yields of the individual gaseous products from the second pyrolysis against $T_{py,1}$. There are trends common among the char-1 samples from different starting fuels. The yields of CO, CO_2, H_2O and C_1-C_2 hydrocarbons decrease with $T_{py,1}$. These trends are explained well by that oxygen-containing functional groups and aliphatic groups of the fuels were decomposed more extensively at higher $T_{py,1}$. It is also seen that the CO yield from the mallee char-1 is clearly higher than those for the other fuels. It was believed that the mallee char-1 retained more oxygen-containing functionalities than the others at the equivalent $T_{py,1}$.

It is also noted for the all feedstock that H_2 yields from the char-1's are nearly steady over the range of $T_{py,1}$ of 450–650 °C. This trend is in contrast to that for the other hydrogen-containing gases, *i.e.*, H_2O and C_1-C_2 hydrocarbons. It is believed that H_2 was formed mainly by condensation between aromatic rings[23,24] and their growth in the ring size. Aliphatic to aromatic carbon conversion is another possible reaction that can form H_2.[25,26] It is, however, unlikely that such a reaction contributed largely to H_2 formation, because it contradicted with decreasing yields of C_1-C_2 hydrocarbons with $T_{py,1}$. Reaction between the carbonaceous char matrix with *in-situ* generated H_2O, *i.e.*, self-gasification of char with steam, could also take place, but decreasing H_2O yield and unchanged H_2 yield from the second pyrol-

ysis were not consistent with each other. It is thus implausible that such self-gasification was an important contributor to the H_2 formation.

The nearly steady yield of H_2 over $T_{py,1}$ of 450–650 °C strongly suggested that the amount of peripheral aromatic carbon bonded to H per mass of char-1 was maintained over this temperature range. In other words, condensation between aromatic rings occurred to a very limited degree. Such little progress of condensation of aromatic rings at $T_{py,1}$ = 450–650 °C implied preservation of aromatic ring systems (ARS's) in size, which were precursors of aromatic compounds, and then their steady emission during the second pyrolysis. However, such an implication was not the case. The emission decreased with increasing $T_{py,1}$, as demonstrated in the next section.

3.2. Emission of Aromatics during the Second Pyrolysis. Figure 6 presents the yields of aromatic compounds from the second pyrolysis of char-1 samples. Table 5 lists the yields of benzene for reference. Benzene was the most abundant aromatic compound except a condition: pine char-1; $T_{py,1}$ = 700 °C. For investigating the emission of aromatics during the second pyrolysis, $T_{py,1}$ was extended to 700 °C for the char-1's from the biomass and 750 °C for the lignite char-1. Figure 6 shows that both yields of the mono-aromatic hydrocarbons (BTXES) and the other aromatics (tar) are 10^{-3} to 10^{-1} wt%-char-1 regardless of the original feedstock and $T_{py,1}$. It is also seen that these yields decrease monotonously with $T_{py,1}$. The yields decrease by two orders of magnitudes with $T_{py,1}$ increasing from 450 to 700 °C for the biomass or 500 to 750 °C for the lignite. Such decrease was attributed to three different chemical events, which occurred simultaneously during the first pyrolysis, namely, (1) decreased concentration of "breakable" linkages between ARS's during the second pyrolysis, (2) increased concentration of linkages between ARS's, and (3) decreased concentration of H that was available in stabilization of radicals formed during the second pyrolysis. Progress of the first pyrolysis by raising $T_{py,1}$ decreases the concentration of residual "breakable" bonds between ARS's, which are mandatory for their release as aromatic compounds into the gas phase. In general, increase in the concentration of inter-ARS linkages

makes the release of aromatics from the char matrix as a macromolecular network more difficult. The release of an aromatic ring system (as an aromatic compound) from the char needs not only breakage of one or more inter-ARS linkages but also subsequent stabilization of radicals formed at ARS, and therefore, requires H, or otherwise, small species such as $\cdot CH_3$ radicals available for capping the radicals. As mentioned in the previous section, condensation between ARS's (*i.e.*, between aromatic C-H's) forming H_2 were insignificant at $T_{py,1}$ of 450–600 °C. It was hence believed that the formation of inter-ARS linkages was rather caused by decomposition of functional groups such as $–CH_3$ and –OH groups bonded to aromatic carbon.[25-27] The following reactions would be examples of formation of inter-ARS linkages.

$$Ar\text{-}OH + Ar'\text{-}OH \rightarrow Ar\text{-}O\text{-}Ar' + H_2O$$

$$Ar\text{-}CH_3 + Ar'\text{-}OH \rightarrow Ar\text{-}O\text{-}Ar' + CH_4$$

$$Ar\text{-}CH_3 + Ar'\text{-}CH_3 \rightarrow Ar\text{-}CH_2\text{-}Ar' + CH_4$$

Progress of decomposition of functional groups was consistent with a trend seen in Figure 5, *i.e.*, monotonous decrease in the CO, CO_2, H_2O and CH_4 yields by the second pyrolysis. The loss of –OH is also suggested by decrease in the yield of phenols (Figure 6(c)) with $T_{py,1}$, which is steeper than those of BTXES and tar. Loss of functional groups as light gas precursors would be associated with that of the available H, of which candidate would be H bonded to aliphatic carbon and hydroxylic H. As shown in Table 1, atomic H/C ratios of the char-1's decrease from 0.64 to 0.40, 0.62 to 0.40, 0.53 to 0.36 for the cedar, pine and mallee, respectively, with increasing $T_{py,1}$ from 450 to 600 °C. The loss of H by increasing $T_{py,1}$ would involve that of the available H, while that of H bonded to aromatic carbon was insignificant.

The BTXES and tar yields from the biomass char-1's were in the range of $3 \cdot 10^{-3}$–$8 \cdot 10^{-2}$ wt%-char-1 at $T_{py,1}$ of 450–600 °C, and these were compared with yields of H_2, which were around 1.2 wt%-char-1 (*see* Figure 5). Under a reasonable assumption that H_2 was formed exclusively from H bonded to aromatic carbon, the corresponding amount of which was estimated to be as much as 14 wt%-char-1 according to a simple calculation as $1.2 \times 12.01/1.008 = 14$ (12.01 and 1.008 are the atomic masses of C and H, respectively). Compared with this amount, the total amount of BTXES and tar, in the range of $3 \cdot 10^{-3}$–$8 \cdot 10^{-2}$ wt%-char-1, was negligibly small. Then, it is said that an extremely small portion of the aromatic C-H was allowed to escape from the char-1, and the portion decreased with $T_{py,1}$ from 450 to 600 °C due to the chemical events as mentioned above. Thus, the abundance of aromatic C-H was not necessarily a measure for the amount of the tar precursors in the char-1. The maintenance of abundance of aromatic C-H, which is shown in Figure 5, was not a measure for the emission of BTXES and tar.

The total tar yields from the biomass char-1 samples were as low as $8 \cdot 10^{-4}$ to $4 \cdot 10^{-3}$ wt%-char-1 with $T_{py,1}$ = 700 °C, but it was also difficult to fully eliminate the tar precursors by the first pyrolysis. The pyrolysis of biomass for producing bio-oil is normally operated at temperature at 500–550 °C so that the bio-oil yield is maximized by minimizing its secondary cracking.[28-31] The second pyrolysis of the char-1 samples with $T_{py,1}$ = 500 °C and 550 °C formed tar with yields of 0.01–0.04 and 0.006–0.03 wt%-dry-char-1, respectively. If tar emission at such level is acceptable, production of char nearly free from tar and that of bio-oil are compatible with each other.

3.3. Emission of Aromatic Hydrocarbons during the Second Pyrolysis. Figure 7 shows the yields of aromatic hydrocarbons (AH) with number of double bonds (d.b.) ranging from 3 to 12 as a function of $T_{py,1}$. Typical or representative aromatic compounds of 3–12 d.b. are listed in Figure 8. It is clearly seen that the yield largely depends on d.b. For the char-1's from the pine and lignite, the 12 d.b. AH yield was smaller by 5–6 orders of magnitude than the 3 d.b. AH yield. Such a ratio could not be calculated for the char-1's from the mallee and cedar because no AH with 9–12 d.b. and 10–12 d.b. were

not detected in the tars from the mallee/cedar char-1's regardless of $T_{py,1}$. For the mallee char-1, the 8 d.b. to 3 d.b. ratio in the AH yield was around $1 \cdot 10^{-3}$. The 9 d.b. to 3 d.b. ratio for the char-1 from the cedar was in a range of $4 \cdot 10^{-6}$–$8 \cdot 10^{-5}$. Thus, the d.b., in other words, the size/shape of ARS's, remarkably influenced their release from the char-1 during the second pyrolysis. This trend would be arisen from that greater ARS's had more linkages to others in a statistic sense. For example, the number of peripheral aromatic carbon of the 3 d.b. ARS's is 6, while that of 12 d.b. ARSs is 12. Release of an ARS would become much more difficult even if the number of linkages increased by one. Much more abundance of smaller ARS's than greater ones was another idea to explain the significant influence of d.b. on the yield of AH. This idea was, however, unlikely when the atomic H/C ratios of the char-1's of 0.4–0.6 at $T_{py,1}$ = 450–600 °C was taken into consideration. The H/C ratios of 0.6 and 0.4 correspond to that of 8 d.b. aromatics (*e.g.*, pyrene with $C_{16}H_{10}$ and H/C ratio of 0.625) and 15 d.b. aromatics (*e.g.*, tricyclopenta[bc,hi,no]coronene with $C_{30}H_{12}$ and H/C ratio of 0.40), respectively. Much more abundance of smaller ARS's such as those with 3 d.b. in the char-1 than greater ones was implausible, unless the char-1's had an extreme composition of ARS's; such as 3 d.b. ARS's and huge ARS's.

Figure 9 shows the yields AH's with 3–12 d.b. from the second pyrolysis of the char-1's with $T_{py,1}$ = 550 °C. The AH yields for every feedstock have been normalized by that of 3 d.b. AH. The normalized yields of 3–8 d.b. AH's for the pine, cedar and mallee are similar to one another, while those of 9–12 d.b. AH's are largely different. No AH's with more than 10 d.b. were detected from the second pyrolysis of the char-1 from the cedar, and no AH's with more than 8 d.b. from the char-1 from the mallee. These trends may be explained by difference in the distribution of ARS in size among the char-1's from the pine, cedar and mallee, although the average size of ARS seemed to be similar to one another according to very similar H/C ratios of the char-1's. The normalized AH yields for the pine are similar to those for the lignite over the range from 3–12 d.b. The compositions of ARS's in these original fuels

are largely different, but nonetheless, the char-1's resulting from the first pyrolysis had similar compositions of ARS's as precursors of aromatics.

Figure 10 shows the yields of 5, 6, 7 and 8 d.b. AH's, which have been normalized by that of 3 d.b. AH's, *i.e.*, BTX and ethylbenzene. It is seen for the cedar, mallee and pine that changes in the normalized AH yields are insignificant at $T_{py,1}$ of 450–600 °C, but their increases are significant at 600–700 °C. Maintenance of the relative yields of 5, 6, 7 and 8 d.b. AH's at $T_{py,1}$ = 450–600 °C was consistent with little progress of condensation of ARS's loosing aromatic C-H's at $T_{py,1}$ = 450–600 °C during the first pyrolysis. On the other hand, the increases in the relative yields at would be due to the progress of such condensation at $T_{py,1}$ = 600–700 °C, which caused growth of ARS's in size, at least transformation of mono-aromatic ring systems to greater ARS's. It is also noted in Figure 10 that the extent of increase in the relative yield at $T_{py,1}$ = 600–700 °C depends both on the d.b. and the original fuel. These dependency would be attributed to the size distribution of ARS's of the char-1's of the fuels, although it is impossible to consider such a variety of the dependency on a quantitative basis.

3.4. Emission of Alkylated and Oxygen-containing Aromatic Compounds during the Second Pyrolysis.

Figure 11 presents the mass-based share of alkyl-substituted AH's in 3, 5, 7 and 8 db AH's. As expected from monotonous decrease with $T_{py,1}$ of the yields of C_1-C_2 hydrocarbon gases from the second pyrolysis (Figure 5), the alkylated AH's became less abundant compared with non-substituted ones as $T_{py,1}$ increased. However, for 3 d.b. and 7 d.b. AH's, the share of alkylated (exactly, mono- or poly-methylated) AH's seems to reach a bottom and/or even increase at $T_{py,1}$ = 650–750 °C. It is difficult to explain these trends, but there could be a possibility of that relatively strong inter-ARS's linkages such as Ar-CH_2-Ar'were broken to newly form methyl groups such as Ar-CH_3 or Ar'-CH_3 at $T_{py,1}$ > 600 °C during the first pyrolysis.

In Figure 12, the share of oxygen-containing aromatics in the aromatics with 3, 4, 5 and 6 d.b. is plotted against $T_{py,1}$. For the 3 d.b. and 5 d.b. aromatic compounds, the oxygen-containing ones are phenols and naphthols, respectively, while those for the 4 d.b. and 6 d.b. aromatics are benzofurans and dibenzofuran, respectively. The abundances of oxygen-containing 3 d.b. and 4 d.b. aromatics decreases with $T_{py,1}$ up to 650 °C, but increases at higher temperature. The increases for the 3 d.b. and 4 d.b. aromatics could be due to formation of aromatic hydroxyls (by decomposition of aromatic ethers) and that of a furanic structure, respectively. However, another possibility, that is, formation of oxygen-containing groups by air oxidation of char-1 during its storage between the first and second pyrolyses. The relatively stable share of dibenzofurans in the 6 d.b. aromatics suggests their thermal stability as high as 6 d.b. AH's.

4. CONCLUSIONS

The following conclusions have been drawn from results within the range of the present experimental conditions.

(1) The pyrolysis of all selected feedstock at $T_{py,1}$ = 450–600 °C produces chars with total volatile matter contents of 10–30 wt% and residual tar contents less than 10^{-1} wt%.

(2) The pyrolysis with $T_{py,1}$ = 600 °C produces chars with residual tar contents of about 10^{-2} wt% or lower.

(3) The char from the pyrolysis with $T_{py,1}$ = 450–700 °C releases aromatic compounds with 3 to 12 d.b., the emission of which ranges from $4 \cdot 10^{-8}$ to $8 \cdot 10^{-2}$ wt%.

(4) Increasing $T_{py,1}$ decreases the emission of tar, but $T_{py,1}$ higher than 700 °C is needed to decrease the tar emission below 10^{-3} wt%.

(5) The ring size distribution of aromatic compounds released from the char is maintained if it has been prepared by pyrolysis at $T_{py,1}$ = 450–600 °C, but the distribution shifts toward greater size at higher $T_{py,1}$.

In addition to its importance to development of tar-free biomass fuel for advanced power generation systems, this study also offers insights that are relevant to use of biochar in soil amendment and carbon storage, and these aspects will be investigated in subsequent studies.

AUTHOR INFORMATION

Corresponding Author

* Tel.: +81 92 583 7796. fax.: +81 92 583 7793. E-mail: junichiro_hayashi@cm.kyushu-u.ac.jp.

ACKNOWLEDGMENT

The authors are also grateful to the Funding Program for the Next Generation World-Leading Researchers (NEXT Program) established by the Japan Society for the Promotion of Science (JSPS). A part of this work was carried out under financial support by The Japan Society for Promotion of Science (JST) in a Program of Strategic Funds for the Promotion of Science and Technology.

REFERENCES

(1) Abdullar, H.; Wu, H. *Energy Fuels* **2009**, *23*, 4174–4181.

(2) Mašek, O.; Brownsort, P.; Cross, A.; Sohi, S. *Fuel* **2013**, *103*, 151–155.

(3) Singh, B. P.; Cowie, A. L.; Smernik, R. *J. Environ. Sci. Technol*. **2012**, *46*, 11770–11778.

(4) Lehmann J.; Joseph S. Biochar for environmental management: science and technology. Earthscan: London, 2009.

(5) Huang, Y.; Kudo, S.; Norinaga, K.; Amaike, M.; Hayashi, J.-i. *Energy Fuels* **2012**, *26*, 256–264.

(6) Huang, Y.; Kudo, S.; Mašek, O, Norinaga, K.; Hayashi, J.-i. *Energy Fuels* **2013**, *27*, 247–254.

(7) Milne, T.; Evans, R. J. 'Biomass gasifier tars: their nature, formation, and conversion' in National Renewable Energy Laboratory Report 1998, NREL/TP-570–25357.

(8) Han, J.; Kim, H. *Renew. Sust. Energ. Rev*. **2008**, *12*, 397–416.

(9) Anis, S.; Zainal, Z. A. *Renew. Sust. Energ. Rev*. **2011**, *15*, 2355–2377.

(10) Richardson, Y.; Blin, J.; Julbe, A. *Prog. Energy Combust. Sci*. **2012**, *38*, 765–781.

(11) Abu El-Rub, Z. Y.; Bramer, E. A.; Brem, G. *Ind. Eng. Chem. Res*. **2004**, *43*, 6911–6919.

(12) Devi, L.; Ptasinski, K. J.; Janssen, F. J. J. G. *Biomass Bioenerg*. **2003**, *24*, 125–140.

(13) Panth, D.; Choi, B.; Tsutsumi, A. 'A novel type of micro-tubular SOFC for application in super IGFC system' in Proc. *Intl. Symp. Chem. Reaction Eng*., Maastricht, 2012.

(14) Li, C.-Z. *Fuel* **2007**, *86*, 1664–1683.

(15) Jamil, K.; Hayashi, J.-i.; Li, C.-Z. *Fuel* **2004**, *83*, 833–843.

(16) Mašek, O.; Hosokai, S.; Norinaga, K.; Li, C.-Z.; Hayashi, J.-i. *Energy Fuels* **2009**, *23*, 4496–4501.

(17) Cao, D.; Sun, Y.; Wang, G. *J. Power Sources* **2007**, *167*, 250–257.

(18) Mathuvel, M.; Jin, X.; Botte, G. G. Encyclopedia of Electrochemical Power Sources **2009**, *3*, 158–171.

(19) Okuno, T.; Sonoyama, S.; Hayashi, J.-i.; Li, C.-Z.; Sathe, C.; Chiba, T. *Energy Fuels* **2005**, *19*, 2164–2171.

(20) Keiluweit, M.; Kleber, M.; Sparrow, M. A.; Simoneit, B. R. T.; Prahl, F. G. *Environ. Sci. Technol.* **2012**, *46*, 9333–9341.

(21) Freddo, A.; Cai, C.; Reid, B. *J. Environ. Pollut*. **2012**, *171*, 18–24.

(22) Hayashi, J.-i.; Iwatsuki, M.; Morishita, K.; Tsutsumi, A.; Li, C.-Z.; Chiba, T. *Fuel* **2002**, *81*, 1977–1987.

(23) Porada, S. *Fuel* **2004**, *83*, 1191–1196.

(24) Hayashi, J.-i.; Takahashi, H.; Doi, S.; Kumagai, H.; Chiba, T.; Yoshida, T.; Tsutsumi, A. *Energy Fuels* **2000**, *14*, 400–408.

(25) Solomon, P. R.; Hamblen, D. G.; Yu, Z.-Z.; Serio, M. A. *Fuel* **1990**, *69*, 754–763.

(26) Solomon, P. R.; Hamblen, D. G.; Carangelo, R. M.; Serio, M. A.; Deshpande, G. V. *Energy Fuels* **1988**, *2*, 405–422.

(27) Mae, K.; Maki, T.; Miura, K. *J. Chem. Eng. Jpn* **2002**, *35*, 778–785.

(28) Scott, D. S.; Piskorz, J.; Radlein, D. *Ind. Eng. Chem. Proc. Des. Dev.* **1985**, *24*, 581–586.

(29) Mohan, D.; Pittman Jr., C.U.; Steele, P.H. *Energy Fuels* **2006**, *20*, 848–889.

(30) Radlein, D. The Production of Chemicals from Fast Pyrolysis Bio-oils. In Fast Pyrolysis of

Biomass: A Handbook; Bridgwater et al., Eds.; CPL Press: Newbury, U.K., 1999, 164–188.

(31) Garcia-Perez, M.; Wang, S.; Shen, J.; Rhodes, M.; Lee, W.J.; Li, C.-Z. *Energy Fuels* **2008**, *22*, 2022–2032.

TABLE Captions

Table 1. Elemental compositions of original fuels and char-1's.

Table 2. Aromatic and non-aromatic compounds formed by second pyrolysis of char-1 derived from pine and detected/quantified by GC/MS.

Table 3. C_4-C_6 non-aromatic compounds, methylfurans and cyclopentadienes detected by pyrolysis-GC/MS of pine chars

Table 4. Reproducibility of quantification of aromatic compounds by pyrolysis-GC/MS. The numbers indicated in this table are the ratios of the minimum yield to maximum one for the individual combinations of aromatic compounds, type of char–1 and $T_{py,1}$.

Table 5. Benzene yield from second pyrolysis of char-1.

FIGURE Captions

Figure 1. Selected ion chromatograms for quantification of coronene ($C_{24}H_{12}$) that was formed by the second pyrolysis of lignite char-1-550.

Figure 2. Effects of $T_{py,1}$ on the yields of (a) char-1 and (b) liquid (tar and water).

Figure 3. Relationship between total gas yield (non-condensable gases and water) and total volatile matter yield from char-1 for the second pyrolysis.

Figure 4. Char-2 yield as a function of $T_{py,1}$.

Figure 5. Yields of gaseous products from the second pyrolysis as a function of $T_{py,1}$.

Figure 6. Effects of $T_{py,1}$ on the yields of BTXES (benzene, toluene, xylenes, ethylbenzene and styrene), tar, phenols (phenol, cresols, xylenols, 2-methoxyphenol and 2-methoxy-4-methylphenol) and polyaromatic compounds (indene and aromatic hydrocarbons and oxygenates that have 5–12 double bonds per molecule) from the second pyrolysis.

Figure 7. Yields of individual aromatic hydrocarbon homologues from the second pyrolysis of char-1. "db" indicates the number of double bonds per molecule. No oxygen-containing compounds such as phenol, cresols, xylenols, naphthols, benzofuran and dibenzofuran are involved in the homologues.

Figure 8. Examples of aromatic compounds with 3–12 double bonds per molecule.

Figure 9. Change in the yield of aromatic hydrocarbon from the second pyrolysis at $T_{py,1}$ = 550 °C as a function of number of double bonds per molecule (d.b.). The yield has been normalized by that of 3 d.b. aromatic hydrocarbon for every char-1.

Figure 10. Effects of $T_{py,1}$ on yields of 5–8 db aromatic hydrocarbons relative to that of 3 db aromatic hydrocarbons from the second pyrolysis of char-1.

Figure 11. Effects of $T_{py,1}$ on mass fractions of alkyl-substituted aromatic hydrocarbons in 3, 5, 7 and 8 db aromatic hydrocarbons.

Figure 12. Effects of $T_{py,1}$ on mass fractions of oxygen-containing aromatics in 3, 4, 5 and 6 db aromatic compounds. 3-db-OH; 3 db aromatics with one or two hydroxylic groups, 4-db-O: benzofurans, 5-db-OH; naphthols, 6-db-O; dibenzofurans.

Table 1. Elemental compositions of original fuels and char-1's.

fuel	T_{py1}, °C	C	H	N	O+S (by diff.)	atomic H/C ratio
		wt%-daf				
cedar	feedstock	50.9	6.2	0.15	42.8	1.45
	450	74.9	4.0	0.16	20.9	0.64
	500	78.9	3.3	0.17	17.6	0.50
	550	79.9	3.3	0.18	16.6	0.49
	600	85.4	2.9	0.17	11.6	0.40
	700	90.0	2.0	0.19	7.9	0.27
pine	feedstock	51.4	5.9	0.15	42.6	1.45
	450	75.0	3.9	0.16	20.9	0.62
	500	78.6	3.5	0.17	17.8	0.53
	550	81.9	3.2	0.18	14.7	0.46
	600	86.5	2.9	0.18	10.5	0.40
	700	91.1	2.2	0.19	6.6	0.29
mallee	feedstock	50.6	6.0	0.13	43.3	1.41
	450	71.4	3.2	0.13	25.3	0.53
	500	75.8	2.9	0.14	21.1	0.46
	550	79.1	2.7	0.19	18.0	0.41
	600	83.9	2.5	0.16	13.4	0.36
	700	90.9	2.0	0.17	7.0	0.26
lignite	feedstock	69.2	4.7	0.60	25.5	0.81
	500	74.5	3.3	0.75	21.4	0.52
	550	76.6	3.0	0.76	19.7	0.46
	600	79.7	2.7	0.77	16.9	0.40
	650	82.6	2.3	0.77	14.1	0.33
	750	87.4	1.6	0.66	10.3	0.22

Table 2. Aromatic and non-aromatic compounds formed by second pyrolysis of char-1 derived from pine and detected/quantified by GC/MS.

number (detected)	number (quantified)	compound	formula	db[b]	relative peak area to benzene		determination/assumption of MS sensitivity
					char-1-450	char-1-600	
1	1	benzene[a]	C_6H_6	3	1.00	1.00	Determined experimentally.
2		2-butanone, 3-methyl-	$C_5H_{10}O$		$1.47\cdot10^{-3}$	0.00	
3		furan, 2,5-dimethyl-	C_6H_8O		$6.15\cdot10^{-3}$	0.00	
4		3-penten-2-one	C_5H_8O		$2.88\cdot10^{-3}$	0.00	
5		furan, 2,4-dimethyl-	C_6H_8O		$1.01\cdot10^{-3}$	0.00	
6		furan, 2,4-dimethyl-	C_6H_8O		$1.01\cdot10^{-3}$	0.00	
7		3-buten-2-one, 3-methyl-	C_5H_8O		$7.97\cdot10^{-4}$	0.00	
8		2-penten-1-ol, 2-methyl-	$C_6H_{12}O$		$5.71\cdot10^{-3}$	$2.54\cdot10^{-2}$	
9		acetic acid	$C_2H_4O_2$		$3.41\cdot10^{-2}$	0.00	
10	2	toluene	C_7H_8	3	$5.52\cdot10^{-1}$	$1.71\cdot10^{-1}$	Determined experimentally.
11		furan, 2-ethyl-5-methyl-	$C_7H_{10}O$		$1.94\cdot10^{-3}$	0.00	
12		3-penten-2-one, (e)-	C_5H_8O		$2.12\cdot10^{-3}$	0.00	
13		furan, 2,3,5-trimethyl-	$C_7H_{10}O$		$1.33\cdot10^{-3}$	0.00	
14		3-hexyne-2,5-diol	$C_6H_{10}O_2$		$2.16\cdot10^{-3}$	0.00	
15		cyclopentanone	C_5H_8O		$3.71\cdot10^{-3}$	$4.08\cdot10^{-3}$	
16	3	ethylbenzene	C_8H_{10}	3	$1.63\cdot10^{-2}$	$3.02\cdot10^{-3}$	Determined experimentally.
17	4	*m,p*-xylene	C_8H_{10}	3	$1.51\cdot10^{-1}$	$1.81\cdot10^{-2}$	Determined experimentally.
18		3,5-hexadien-1-ol, (z)-	$C_6H_{10}O$		$1.06\cdot10^{-3}$	0.00	
19	5	*o*-xylene	C_8H_{10}	3	$2.78\cdot10^{-2}$	$4.84\cdot10^{-3}$	Determined experimentally.
20	6	styrene	C_8H_8	4	$3.41\cdot10^{-2}$	$1.46\cdot10^{-2}$	Determined experimentally.
21		2-cyclopenten-1-one	C_5H_6O		$1.57\cdot10^{-2}$	$1.26\cdot10^{-3}$	
22		benzene, methoxy-	$C_9H_{12}O$	3	$2.97\cdot10^{-3}$	0.00	
23		benzene, propyl-	C_9H_{12}	3	$2.27\cdot10^{-3}$	0.00	

24		benzene, 1-ethyl-2-methyl-	C_9H_{12}	3	$9.97 \cdot 10^{-3}$	0.00	
25		benzene, 1,3,5-trimethyl-	C_9H_{12}	3	$6.06 \cdot 10^{-3}$	$1.43 \cdot 10^{-3}$	
26		2-cyclopenten-1-one, 2-methyl-	C_6H_8O		$8.28 \cdot 10^{-3}$	$1.12 \cdot 10^{-3}$	
27		benzene, 1-methylethyl-	C_9H_{12}	3	$2.10 \cdot 10^{-3}$	0.00	
28		2-cyclopenten-1-one, 3,4-dimethyl-	$C_7H_{10}O$		$1.93 \cdot 10^{-3}$	0.00	
29		α-methylstyrene	C_9H_{10}	4	$3.39 \cdot 10^{-3}$	$1.68 \cdot 10^{-3}$	
30		benzene, 1,3,5-trimethyl-	C_9H_{12}	3	$1.35 \cdot 10^{-2}$	0.00	
31		2-cyclopenten-1-one, 2,3-dimethyl-	$C_7H_{10}O$		$7.49 \cdot 10^{-4}$	$2.06 \cdot 10^{-3}$	
32		indane	C_9H_{10}	3	$9.86 \cdot 10^{-3}$	$2.02 \cdot 10^{-3}$	
33		benzaldehyde	C_7H_6O	3	$2.19 \cdot 10^{-3}$	0.00	
34	7	benzofuran	C_8H_6O	4	$2.48 \cdot 10^{-1}$	$2.60 \cdot 10^{-2}$	Determined experimentally.
35		cis-β-methylstyrene	C_9H_{10}	4	$1.34 \cdot 10^{-3}$	$1.27 \cdot 10^{-3}$	
36		benzene, 1-methoxy-3-methyl-	$C_8H_{10}O$	3	$9.27 \cdot 10^{-3}$	$5.15 \cdot 10^{-3}$	
37		benzene, 1-methoxy-4-methyl- or 3-methyl-	$C_8H_{10}O$	3	$1.31 \cdot 10^{-3}$	0.00	
38		2-cyclopenten-1-one, 3-methyl-	C_6H_8O		$1.02 \cdot 10^{-3}$	0.00	
39		2-cyclopenten-1-one, 2,3-dimethyl-	$C_7H_{10}O$		$7.17 \cdot 10^{-3}$	$1.18 \cdot 10^{-3}$	
40	8	indene	C_9H_8	4	$3.81 \cdot 10^{-2}$	$1.74 \cdot 10^{-2}$	Determined experimentally.
41		2-cyclopenten-1-one, 3,4-dimethyl-	$C_7H_{10}O$		$9.18 \cdot 10^{-4}$	0.00	
42		benzene, 1-ethyl-2,4-dimethyl-	$C_{10}H_{14}$	3	$3.26 \cdot 10^{-4}$	0.00	
43		benzene, 1-methyl-3-(1-methylethyl)-	$C_{10}H_{14}$	3	$1.12 \cdot 10^{-3}$	0.00	
44		benzene, (2-methyl-2-propenyl)- (2-allyltoluene)	$C_{10}H_{12}$	3	$1.13 \cdot 10^{-3}$	0.00	
45		benzene, 4-ethenyl-1,2-dimethyl-	$C_{10}H_{12}$	3	$1.47 \cdot 10^{-3}$	0.00	
46		benzaldehyde, 2-hydroxy-	$C_7H_6O_2$	3	$1.24 \cdot 10^{-3}$	0.00	
47		2-cyclopenten-1-one, 2,3-dimethyl-	$C_7H_{10}O$		$1.84 \cdot 10^{-3}$	0.00	
48		benzofuran, 7-methyl-	C_9H_8O	4	$1.40 \cdot 10^{-2}$	0.00	
49		2-propenal, 3-phenyl- (cinnamal-dehyde)	C_9H_8O	4	$2.05 \cdot 10^{-2}$	$1.43 \cdot 10^{-3}$	
50		acetophenone	C_8H_8O	3	$2.41 \cdot 10^{-3}$	0.00	

51	9	benzofuran, 2-methyl-	C_9H_8O	4	$1.29 \cdot 10^{-1}$	$1.45 \cdot 10^{-2}$	Determined experimentally.
52	10	phenol	C_6H_6O	3	$4.02 \cdot 10^{-1}$	$4.32 \cdot 10^{-2}$	Determined experimentally.
53		benzaldehyde, 3-methyl-	C_8H_8O	3	$1.03 \cdot 10^{-3}$	$1.08 \cdot 10^{-3}$	
54	11	phenol, 2-methoxy-	$C_7H_8O_2$	3	$4.35 \cdot 10^{-2}$	0.00	Determined experimentally.
55		2-methylindene	$C_{10}H_{10}$	4	$1.80 \cdot 10^{-3}$	0.00	
56		1h-indene, 3-methyl-	$C_{10}H_{10}$	4	$6.58 \cdot 10^{-3}$	0.00	
57	12	phenol, 2-methyl-	C_7H_8O	3	$1.43 \cdot 10^{-1}$	$5.02 \cdot 10^{-3}$	Determined experimentally.
58	13	phenol, 2,6-dimethyl-	$C_8H_{10}O$	3	$1.64 \cdot 10^{-2}$	0.00	Determined experimentally.
59		1,3-benzodioxol-2-one	$C_7H_4O_3$	3	$2.38 \cdot 10^{-3}$	0.00	
60	14	phenol, 3-methyl-	C_7H_8O	3	$3.65 \cdot 10^{-2}$	$4.28 \cdot 10^{-3}$	Determined experimentally.
61	15	phenol, 4-methyl-	C_7H_8O	3	$2.21 \cdot 10^{-2}$	$3.20 \cdot 10^{-3}$	Determined experimentally.
62	16	naphthalene	$C_{10}H_8$	5	$3.11 \cdot 10^{-1}$	$2.76 \cdot 10^{-1}$	Determined experimentally.
63		benzofuran, 4,7-dimethyl-	$C_{10}H_{10}O$	4	$5.40 \cdot 10^{-3}$	0.00	
64		ethyl-2-benzofuran	$C_{10}H_{10}O$	4	$2.47 \cdot 10^{-3}$	0.00	
65		phenol, 2-methoxy-3-methyl-	$C_8H_{10}O_2$	3	$3.81 \cdot 10^{-3}$	0.00	
66		benzofuran, dimethyl- (isomer 1)	$C_{10}H_{10}O$	4	$2.79 \cdot 10^{-3}$	0.00	
67		benzofuran, 2,4-dimethyl- (isomer 2)	$C_{10}H_{10}O$	4	$2.06 \cdot 10^{-2}$	0.00	
68		benzofuran, 2,6-dimethyl- (isomer 3)	$C_{10}H_{10}O$	4	$8.70 \cdot 10^{-4}$	0.00	
69		benzofuran, dimethyl- (isomer 4)	$C_{10}H_{10}O$	4	$1.40 \cdot 10^{-3}$	0.00	
70		benzofuran, dimethyl- (isomer 5)	$C_{10}H_{10}O$	4	$2.53 \cdot 10^{-3}$	0.00	
71	17	phenol, 2-methoxy-4-methyl- (creosol)	$C_8H_{10}O_2$	3	$3.24 \cdot 10^{-3}$	0.00	Determined experimentally.
72	18	phenol, 2,4-dimethyl-	$C_8H_{10}O$	3	$1.55 \cdot 10^{-2}$	$9.24 \cdot 10^{-4}$	Determined experimentally.
73		phenol, 2,4,5-trimethyl-	$C_9H_{12}O$	3	$2.58 \cdot 10^{-3}$	0.00	
74	19	phenol, 2,3-dimethyl-	$C_8H_{10}O$	3	$9.63 \cdot 10^{-3}$	$9.29 \cdot 10^{-4}$	Determined experimentally.
75		phenol, 4-ethyl-	$C_8H_{10}O$	3	$3.42 \cdot 10^{-3}$	0.00	
76		phenol, 3-ethyl-	$C_8H_{10}O$	3	$3.90 \cdot 10^{-3}$	0.00	
77		phenol, 4-ethyl-3-methyl-	$C_9H_{12}O$	3	$7.27 \cdot 10^{-4}$	0.00	
78		3-buten-2-one, 3-methyl-4-phenyl-	$C_{11}H_{12}O$	4	$1.67 \cdot 10^{-3}$	0.00	
79	20	phenol, 3,4-dimethyl-	$C_8H_{10}O$	3	$1.17 \cdot 10^{-3}$	0.00	Determined experimentally.

80	21	naphthalene, 2-methyl-	$C_{11}H_{10}$	5	$1.64 \cdot 10^{-1}$	$2.94 \cdot 10^{-2}$	Determined experimentally.
81		phenol, 2-ethyl-6-methyl-	$C_9H_{12}O$	3	$1.16 \cdot 10^{-3}$	0.00	
82		phenol, 2-methoxy-5-methyl	$C_8H_{10}O_2$	3	$5.34 \cdot 10^{-4}$	$1.56 \cdot 10^{-3}$	
83		phenol, 4-ethyl-2-methoxy- (*p*-ethylguaiacol)	$C_9H_{12}O_2$	3	$5.02 \cdot 10^{-4}$	0.00	
84		phenol, 2-ethyl-5-methyl-	$C_9H_{12}O$	3	$6.20 \cdot 10^{-3}$	0.00	
85	22	naphthalene, 1-methyl-	$C_{11}H_{10}$	5	$7.64 \cdot 10^{-2}$	$1.26 \cdot 10^{-2}$	Determined experimentally.
86		cinnamaldehyde, β-methyl-	$C_{10}H_{10}O$	4	$1.10 \cdot 10^{-3}$	0.00	
87		2-propenal, 3-(4-methylphenyl)-	$C_{10}H_{10}O$	4	$6.79 \cdot 10^{-4}$	0.00	
88		phenol, 2,4,6-trimethyl- (mesitol)	$C_9H_{12}O$	3	$1.12 \cdot 10^{-2}$	0.00	
89		phenol, 2-ethyl-6-methyl-	$C_9H_{12}O$	3	$9.79 \cdot 10^{-3}$	0.00	
90		benzene, 1-ethenyl-4-methoxy- (*p*-methoxystyrene)	$C_9H_{10}O$	4	$2.66 \cdot 10^{-2}$	0.000	
91		phenol, 2-propyl-	$C_9H_{12}O$	3	$5.09 \cdot 10^{-3}$	0.00	
92		phenol, 4-(2-propenyl)- (*p*-allylphenol)	$C_9H_{10}O$	4	$5.20 \cdot 10^{-4}$	0.00	
93		2-methoxy-4-vinylphenol (p-vinylguaiacol)	$C_9H_{10}O_2$	4	$9.29 \cdot 10^{-3}$	$5.34 \cdot 10^{-3}$	
94		2-propenal, 2-methyl-3-phenyl-	$C_{10}H_{10}O$	4	$1.37 \cdot 10^{-3}$	0.00	
95		2-isopropoxyphenol	$C_9H_{12}O_2$	3	$9.10 \cdot 10^{-3}$	0.00	
96		3-penten-2-one, 4-phenyl-	$C_{11}H_{12}O$	4	$1.11 \cdot 10^{-3}$	0.00	
97	23	biphenyl	$C_{12}H_{10}$	6	$5.50 \cdot 10^{-2}$	$3.09 \cdot 10^{-2}$	Determined experimentally.
98		phenol, 2,3,6-trimethyl-	$C_9H_{12}O$	3	$4.12 \cdot 10^{-3}$	0.00	
99		1,1'-biphenyl, 3-methyl-	$C_{13}H_{12}$	6	$1.35 \cdot 10^{-2}$	0.00	
100	24	1-naphthol [b]	$C_{10}H_8O$	5	$1.63 \cdot 10^{-2}$	$2.09 \cdot 10^{-3}$	Determined experimentally.
101		phenol, 2-methoxy-4-propyl-	$C_{10}H_{14}O_2$	3	$1.48 \cdot 10^{-3}$	0.00	
102		benzene, 1-methoxy-4-propyl-	$C_{10}H_{14}O_2$	3	$1.04 \cdot 10^{-3}$	0.00	
103		phenol, 2-methoxy-4-(2-propenyl) (eugenol)	$C_9H_{10}O$	4	$1.56 \cdot 10^{-2}$	0.00	
104		naphthalene, 2,6-dimethyl-	$C_{12}H_{12}$	5	$6.17 \cdot 10^{-3}$	0.00	
105		phenol, 3-ethyl-5-methyl-	$C_9H_{12}O$	3	$3.36 \cdot 10^{-3}$	0.00	
106		phenol, 2-(propenyl)- (2-allylphenol)	$C_9H_{10}O$	4	$9.44 \cdot 10^{-3}$	0.00	
107		naphthalene, 1,4-dimethyl-	$C_{12}H_{12}$	5	$9.02 \cdot 10^{-3}$	0.00	

108		4-isopropenylphenol	$C_9H_{10}O$	4	0.00	$1.52 \cdot 10^{-3}$	
109		naphthalene, 1,6-dimethyl-	$C_{12}H_{12}$	5	$3.27 \cdot 10^{-3}$	0.00	
110		phenol, 3,5-diethyl-	$C_{10}H_{14}O$	3	$4.11 \cdot 10^{-3}$	0.00	
111		1,2-benzenediol, 4-methyl-	$C_7H_8O_2$	3	$6.99 \cdot 10^{-3}$	$1.50 \cdot 10^{-3}$	
112		3-methoxy-5-methylphenol	$C_8H_{10}O_2$	3	$1.37 \cdot 10^{-2}$	0.00	
113		2-methyl-5-hydroxybenzofuran	$C_9H_8O_2$	4	$1.84 \cdot 10^{-2}$	$1.17 \cdot 10^{-3}$	
114		benzaldehyde, dimethyl-	$C_9H_{10}O$	3	$1.98 \cdot 10^{-3}$	0.00	
115		134, benzaldehyde, dimethyl-	$C_9H_{10}O$	3	$2.74 \cdot 10^{-3}$	0.00	
116		134, benzaldehyde, dimethyl-	$C_9H_{10}O$	3	$9.28 \cdot 10^{-4}$	0.00	
117	25	acenaphthylene	$C_{12}H_8$	6	$1.92 \cdot 10^{-2}$	$9.23 \cdot 10^{-3}$	Determined experimentally.
118		diphenylmethane	$C_{13}H_{12}$	6	$7.73 \cdot 10^{-3}$	0.00	
119		phenol, 2-methoxy-4-(1-propenyl)- (isoeugenol)	$C_{10}H_{12}O_2$	4	$1.80 \cdot 10^{-3}$	$1.18 \cdot 10^{-3}$	
120		naphthalene, 2-ethenyl-	$C_{12}H_{10}$	5	$3.41 \cdot 10^{-3}$	0.00	
121		naphthalene, 2,3,6-trimethyl-	$C_{13}H_{14}$	5	$2.11 \cdot 10^{-3}$	$1.33 \cdot 10^{-3}$	
122		naphthalene, 1,6,7-trimethyl-	$C_{13}H_{14}$	5	$9.41 \cdot 10^{-4}$	$1.07 \cdot 10^{-3}$	
123	26	1,3-benzenediol (resorcinol) [c]	$C_6H_6O_2$	3	$7.24 \cdot 10^{-2}$	0.00	Determined experimentally.
124	27	dibenzofuran	$C_{12}H_8O$	6	$1.02 \cdot 10^{-1}$	$5.02 \cdot 10^{-2}$	Determined experimentally.
125		3-(2-methyl-propenyl)-1h-indene	$C_{13}H_{14}$	5	$2.37 \cdot 10^{-3}$	$2.39 \cdot 10^{-3}$	
126		naphthalene, 1,6,7-trimethyl-	$C_{13}H_{14}$	5	$4.25 \cdot 10^{-4}$	0.00	
127		2h-1-benzopyran-2-one (coumarin)	$C_9H_6O_2$	4	$4.45 \cdot 10^{-4}$	0.00	
128		acenaphthenone	$C_{12}H_8O$	5	$1.07 \cdot 10^{-3}$	$5.26 \cdot 10^{-4}$	
129		1h-phenalene	$C_{13}H_{10}$	6	$3.06 \cdot 10^{-4}$	$1.09 \cdot 10^{-2}$	
130	28	fluorene	$C_{13}H_{10}$	6	$2.66 \cdot 10^{-2}$	$1.04 \cdot 10^{-2}$	Determined experimentally.
131		phenol, 4-methyl-2,6-dimethoxy (syringgol)	$C_9H_{12}O_3$	3	$1.63 \cdot 10^{-3}$	$1.95 \cdot 10^{-3}$	
132		dibenzofuran, methyl- (isomer 1)	$C_{13}H_{10}O$	6	$4.85 \cdot 10^{-3}$	$9.16 \cdot 10^{-4}$	
133		dibenzofuran, methyl- (isomer 2)	$C_{13}H_{10}O$	6	$5.63 \cdot 10^{-3}$	$1.60 \cdot 10^{-3}$	
134		dibenzofuran, methyl- (isomer 3)	$C_{13}H_{10}O$	6	$1.91 \cdot 10^{-3}$	$9.90 \cdot 10^{-3}$	
135		dibenzofuran, methyl- (isomer 4)	$C_{13}H_{10}O$	6	$2.10 \cdot 10^{-3}$	0.00	
136		fluorene, methyl- (isomer 1)	$C_{14}H_{12}$	6	$7.46 \cdot 10^{-4}$	0.00	

137		fluorene, methyl- (isomer 2)	$C_{14}H_{12}$	6	$1.31 \cdot 10^{-3}$	0.00	
138		fluorene, methyl- (isomer 3)	$C_{14}H_{12}$	6	$4.47 \cdot 10^{-4}$	$1.07 \cdot 10^{-3}$	
139		fluorene, methyl- (isomer 4)	$C_{14}H_{12}$	6	$5.83 \cdot 10^{-4}$	$2.26 \cdot 10^{-3}$	
140		naphtho[2,1-b]furan, 1,2-dimethyl-	$C_{14}H_{12}O$	6	$1.15 \cdot 10^{-3}$	$2.88 \cdot 10^{-3}$	
141		naphthol, methyl- (isomer 1)	$C_{11}H_{10}O$	5	0.00	$2.82 \cdot 10^{-3}$	
142		naphthol, methyl- (isomer 2)	$C_{11}H_{10}O$	5	0.00	$2.27 \cdot 10^{-3}$	
143		naphthol, methyl- (isomer 3)	$C_{11}H_{10}O$	5	0.00	$1.27 \cdot 10^{-3}$	
144		naphthol, methyl- (isomer 4)	$C_{11}H_{10}O$	5	0.00	$5.42 \cdot 10^{-3}$	
145		naphthol, methyl- (isomer 5)	$C_{11}H_{10}O$	5	0.00	$3.19 \cdot 10^{-3}$	
146		naphthol, methyl- (isomer 6)	$C_{11}H_{10}O$	5	0.00	$3.38 \cdot 10^{-3}$	
147	29	phenanthrene	$C_{14}H_{10}$	7	$5.31 \cdot 10^{-2}$	$1.95 \cdot 10^{-2}$	Determined experimentally.
148	30	anthracene	$C_{14}H_{10}$	7	$1.68 \cdot 10^{-2}$	$4.04 \cdot 10^{-3}$	Determined experimentally.
149		1-naphthol, 6,7-dimethyl-	$C_{12}H_{12}O$	5	$1.51 \cdot 10^{-3}$	$3.16 \cdot 10^{-3}$	
150		biphenyl-4-ol	$C_{12}H_{12}O$	6	0.00	$4.53 \cdot 10^{-3}$	
151		biphenyl-3-ol	$C_{12}H_{12}O$	6	0.00	$5.10 \cdot 10^{-3}$	
152	31	phenanthrene/anthracene, methyl- (isomer 1)	$C_{15}H_{12}$	7	$5.26 \cdot 10^{-3}$	$1.08 \cdot 10^{-3}$	Sensitivity for 2-methyl-anthracene was given.
153	32	phenanthrene/anthracene, methyl- (isomer 2)	$C_{15}H_{12}$	7	$6.58 \cdot 10^{-3}$	$1.35 \cdot 10^{-3}$	Sensitivity for 2-methyl-anthracene was given.
154	33	anthracene, 2-methyl	$C_{15}H_{12}$	7	$5.26 \cdot 10^{-3}$	$6.64 \cdot 10^{-4}$	Determined experimentally.
155	34	phenanthrene/anthracene, methyl- (isomer 3)	$C_{15}H_{12}$	7	$2.27 \cdot 10^{-3}$	$3.87 \cdot 10^{-4}$	Sensitivity for 2-methyl-anthracene was given.
156	35	phenanthrene/anthracene, methyl- (isomer 4)	$C_{15}H_{12}$	7	$5.94 \cdot 10^{-3}$	$8.02 \cdot 10^{-4}$	Sensitivity for 2-methyl-anthracene was given.
157		naphthalene,2-phenyl-	$C_{16}H_{12}$	8	0.00	$3.75 \cdot 10^{-3}$	
158	36	fluoranthene	$C_{16}H_{10}$	8	$1.33 \cdot 10^{-2}$	$8.61 \cdot 10^{-3}$	Determined experimentally.
159	37	pyrene	$C_{16}H_{10}$	8	$1.13 \cdot 10^{-2}$	$6.47 \cdot 10^{-3}$	Determined experimentally.
160	38	fluoranthene/pyrene, methyl- (isomer 1)	$C_{17}H_{12}$	8	$1.34 \cdot 10^{-3}$	$2.36 \cdot 10^{-4}$	Sensitivity for pyrene was given.
161	39	fluoranthene/pyrene, methyl- (isomer 2)	$C_{17}H_{12}$	8	$4.10 \cdot 10^{-3}$	$8.22 \cdot 10^{-4}$	Sensitivity for pyrene was given.
162	40	fluoranthene/pyrene, methyl- (isomer 3)	$C_{17}H_{12}$	8	$2.82 \cdot 10^{-3}$	$6.17 \cdot 10^{-4}$	Sensitivity for pyrene was given.
163	41	fluoranthene/pyrene, methyl- (isomer 4)	$C_{17}H_{12}$	8	$1.05 \cdot 10^{-3}$	$1.65 \cdot 10^{-4}$	Sensitivity for pyrene was given.

164	42	fluoranthene/pyrene, methyl- (isomer 5)	$C_{17}H_{12}$	8	$8.05 \cdot 10^{-4}$	$1.15 \cdot 10^{-4}$	Sensitivity for pyrene was given.
165	43	fluoranthene/pyrene, methyl- (isomer 6)	$C_{17}H_{12}$	8	$7.35 \cdot 10^{-4}$	$8.75 \cdot 10^{-5}$	Sensitivity for pyrene was given.
166	44	benz[a]anthracene or triphenylene	$C_{18}H_{12}$	9	$3.80 \cdot 10^{-3}$	$7.12 \cdot 10^{-4}$	Determined experimentally.
167	45	chrysene	$C_{18}H_{12}$	9	$3.02 \cdot 10^{-3}$	$6.57 \cdot 10^{-4}$	Sensitivity for chrysene was given.
168	46	non-substituted 10 db aromatic compound (isomer 1)	$C_{20}H_{12}$	10	$3.47 \cdot 10^{-3}$	$5.46 \cdot 10^{-4}$	Sensitivity for benzo[e]pyrene was given.
169	47	non-substituted 10 db aromatic compound (isomer 2)	$C_{20}H_{12}$	10	$1.13 \cdot 10^{-3}$	$1.83 \cdot 10^{-4}$	Sensitivity for benzo[e]pyrene was given.
170	48	non-substituted 10 db aromatic compound (isomer 3)	$C_{20}H_{12}$	10	$1.24 \cdot 10^{-3}$	$1.02 \cdot 10^{-4}$	Sensitivity for benzo[e]pyrene was given.
171	49	benzo[e]pyrene	$C_{20}H_{12}$	10	$1.50 \cdot 10^{-3}$	$2.38 \cdot 10^{-4}$	Determined experimentally.
172	50	non-substituted 10 db aromatic compound (isomer 4)	$C_{20}H_{12}$	10	$2.33 \cdot 10^{-3}$	$3.32 \cdot 10^{-4}$	Sensitivity for benzo[e]pyrene was given.
173	51	non-substituted 10 db aromatic compound (isomer 5)	$C_{20}H_{12}$	10	$3.36 \cdot 10^{-4}$	$3.64 \cdot 10^{-5}$	Sensitivity for benzo[e]pyrene was given.
174	52	non-substituted 11 db aromatic compound (isomer 1)	$C_{22}H_{12}$	11	$9.25 \cdot 10^{-4}$	$1.13 \cdot 10^{-4}$	Sensitivity for benzo[g,h,i]perylene was given.
175	53	non-substituted 11 db aromatic compound (isomer 2)	$C_{22}H_{14}$	11	0.00	$8.62 \cdot 10^{-6}$	Sensitivity for benzo[g,h,i]perylene was given.
176	54	benzo[ghi]perylene	$C_{22}H_{12}$	11	$6.87 \cdot 10^{-4}$	$9.36 \cdot 10^{-5}$	Determined experimentally.
177	55	non-substituted 11 db aromatic compound (isomer 3)	$C_{22}H_{12}$	11	$3.96 \cdot 10^{-4}$	$1.73 \cdot 10^{-5}$	Sensitivity for benzo[g,h,i]perylene was given.
178	56	coronene	$C_{24}H_{12}$	12	0.00	$4.42 \cdot 10^{-6}$	Determined experimentally.
peak-area-basded fraction of quantified 56 compounds in that of detected 178 compounds, %					88.3	93.1	

a) The yields of benzene were 0.0299 and 0.0172 wt%-dry-char-1 at $T_{py,1}$ = 450 °C and 600 °C, respectively.
b) Number of double bonds per molecule (only for aromatic compounds).
c) 2-naphthol is not involved in this table, but it was detected in SIR mode and quantified.
d) 1,2-benzenediol (catechol) is not involved in this table, but it was detected in SIR mode and quantified.

Table 3. C_4-C_6 non-aromatic compounds, methylfurans and cyclopentadienes detected by pyrolysis-GC/MS of pine chars

No.	compounds	formula	relative peak area to benzene [a]	
			$T_{py,1}$ = 450°C	$T_{py,1}$ = 600 °C
1	2-butene	C_4H_8	$1.65 \cdot 10^{-2}$	$1.01 \cdot 10^{-2}$
2	1-butyne	C_4H_6	$2.34 \cdot 10^{-2}$	$2.16 \cdot 10^{-2}$
3	1-propene, 2-methyl-	C_4H_8	$1.83 \cdot 10^{-2}$	$1.28 \cdot 10^{-2}$
4	acetaldehyde	C_2H_4O	$3.25 \cdot 10^{-2}$	$1.34 \cdot 10^{-2}$
5	methanol	CH_4O	$5.52 \cdot 10^{-2}$	$2.91 \cdot 10^{-3}$
6	1-pentene	C_5H_{10}	$2.07 \cdot 10^{-3}$	$3.99 \cdot 10^{-3}$
7	pentadiene (isomer 1)[b]	C_5H_8	$1.40 \cdot 10^{-2}$	$5.54 \cdot 10^{-3}$
8	pentadiene (isomer 2)[b]	C_5H_8	$6.42 \cdot 10^{-3}$	$2.38 \cdot 10^{-3}$
9	pentadiene (isomer 3)[b]	C_5H_8	$4.98 \cdot 10^{-3}$	$7.79 \cdot 10^{-4}$
10	cyclopentene	C_5H_8	$7.80 \cdot 10^{-4}$	0.00
11	1,3-cyclopentadiene	C_5H_6	$2.14 \cdot 10^{-2}$	$1.56 \cdot 10^{-2}$
12	butane	C_4H_{10}	$1.62 \cdot 10^{-2}$	0.00
13	acetic acid, methyl ester	$C_3H_6O_2$	$3.35 \cdot 10^{-3}$	0.00
14	1-hexene	C_6H_{12}	$4.36 \cdot 10^{-3}$	$7.36 \cdot 10^{-3}$
15	acetonitrile	C_2H_3N	$1.38 \cdot 10^{-2}$	$1.42 \cdot 10^{-2}$
16	furan, 2-methyl-	C_5H_6O	$5.10 \cdot 10^{-3}$	0.00
17	furan, 3-methyl-	C_5H_6O	$1.90 \cdot 10^{-3}$	0.00
18	1,3-cyclopentadiene, 1-methyl-	C_6H_8	$9.71 \cdot 10^{-3}$	$2.42 \cdot 10^{-3}$
19	cyclopentene,3-methylene-	C_6H_8	$1.61 \cdot 10^{-3}$	$4.70 \cdot 10^{-4}$
20	methyl vinyl ketone	C_4H_6O	$3.32 \cdot 10^{-3}$	0.00
21	1,3-cyclopentadiene, 5-methyl-	C_6H_8	$1.23 \cdot 10^{-2}$	$2.40 \cdot 10^{-3}$
22	2-butanone	C_4H_8O	$2.32 \cdot 10^{-2}$	$9.06 \cdot 10^{-4}$
23	succinic anhydride	$C_4H_4O_3$	$1.21 \cdot 10^{-4}$	$3.66 \cdot 10^{-4}$
24	4-penten-1-ol, 2-methylene-	$C_6H_{10}O$	$1.30 \cdot 10^{-2}$	$9.05 \cdot 10^{-3}$

a) The yields of benzene were 0.0299 and 0.0172 wt%-dry-char-1 at $T_{py,1}$ = 450 °C and 600 °C, respectively.
b) Three pentadiene isomers were detected.

Table 4. Reproducibility of quantification of aromatic compounds by pyrolysis-GC/MS. The numbers indicated in this table are the ratios of the minimum yield to maximum one for the individual combinations of aromatic compounds, type of char-1 and $T_{py,1}$.

feedstock	compound	pyrolyzed char sample		
		char-1-500	char-1-550	char-1-600
pine	benzene	0.92	0.93	0.90
	phenol	0.89	0.76	0.80
	naphthalene	0.79	0.88	0.87
	phenanthrene	0.80	0.97	0.87
	anthracene	0.80	0.94	0.91
	fluoranthene	0.93	0.81	0.96
	pyrene	0.86	0.73	0.90
	chrysene	0.96	0.60	0.79
	benzo[ghi]perylene	0.64	0.50	0.59
cedar	benzene	0.88	0.99	0.85
	phenol	0.76	0.84	0.98
	naphthalene	0.99	0.93	0.87
	phenanthrene	0.95	0.76	0.65
	anthracene	0.74	0.72	0.99
	fluoranthene	0.77	0.66	0.61
	pyrene	0.82	0.74	0.56
	chrysene	0.66	n.d.	n.d.
	benzo[ghi]perylene	n.d.	0.70	n.d.
mallee	benzene	0.94	0.70	0.76
	phenol	0.94	0.75	0.97
	naphthalene	0.90	0.79	0.75
	phenanthrene	0.82	0.71	0.65
	anthracene	0.63	0.71	0.67
	fluoranthene	0.83	0.79	0.79
	pyrene	0.79	0.68	0.71
	chrysene	n.d.	n.d.	n.d.
	benzo[ghi]perylene	n.d.	n.d.	n.d.
lignite	benzene	0.88	0.98	0.99
	phenol	0.89	0.89	0.94
	naphthalene	0.90	0.98	0.84
	phenanthrene	1.00	0.90	0.78
	anthracene	0.96	0.90	0.90
	fluoranthene	0.96	0.88	0.76
	pyrene	0.96	0.81	0.85
	chrysene	0.81	0.69	0.95
	benzo[ghi]perylene	0.91	0.72	0.96

n.d: not detected.

Table 5. Benzene yield from second pyrolysis of char-1.

$T_{py,1}$, °C	450	500	550	600	650	700	750
cedar	0.045	0.031	0.029	0.022	n.d.	0.0016	n.d.
mallee	0.034	0.023	0.018	0.013	n.d.	0.0013	n.d.
pine	0.030	0.024	0.023	0.017	n.d.	0.0010	n.d.
lignite	n.d.	0.041	0.039	0.025	0.011	n.d.	0.001

Unit; wt%-dry-char-1, n.d.; not determined.

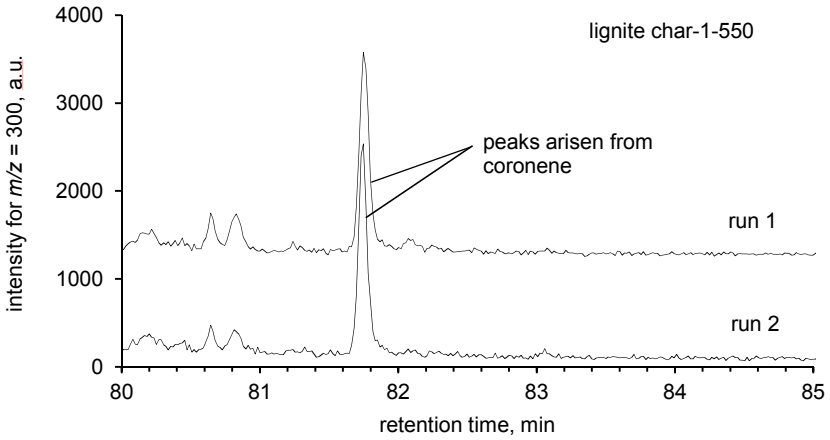

Figure 1. Selected ion chromatograms for quantification of coronene ($C_{24}H_{12}$) that was formed by the second pyrolysis of lignite char-1-550.

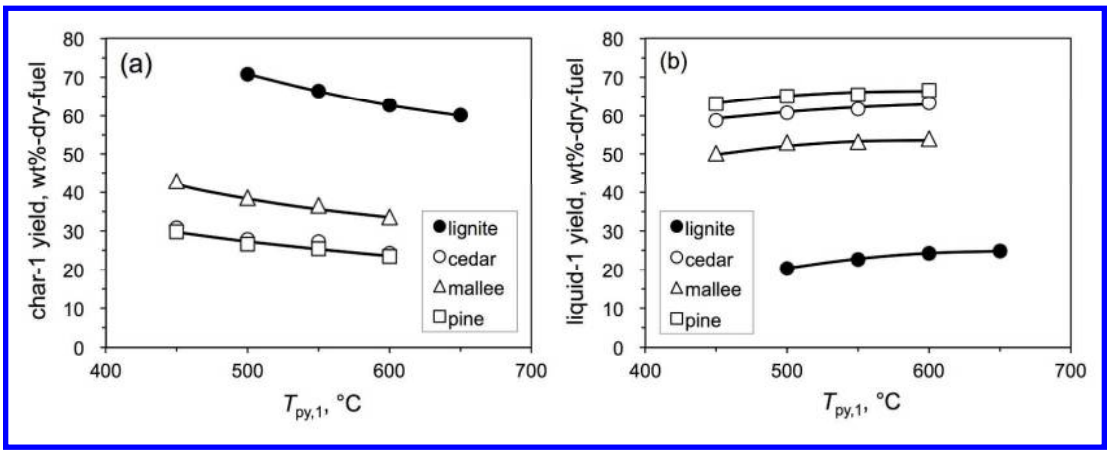

Figure 2. Effects of $T_{py,1}$ on the yields of (a) char-1 and (b) liquid (tar and water).

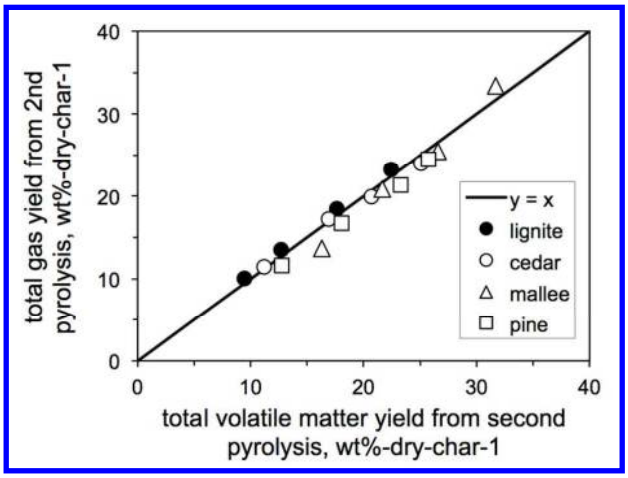

Figure 3. Relationship between total gas yield (non-condensable gases and water) and total volatile matter yield from char-1 for the second pyrolysis.

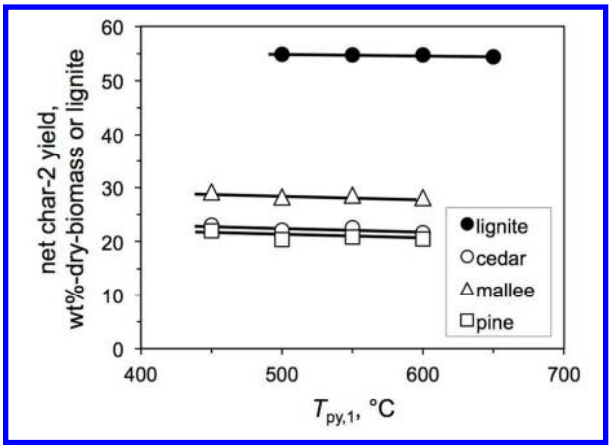

Figure 4. Char-2 yield as a function of $T_{py,1}$.

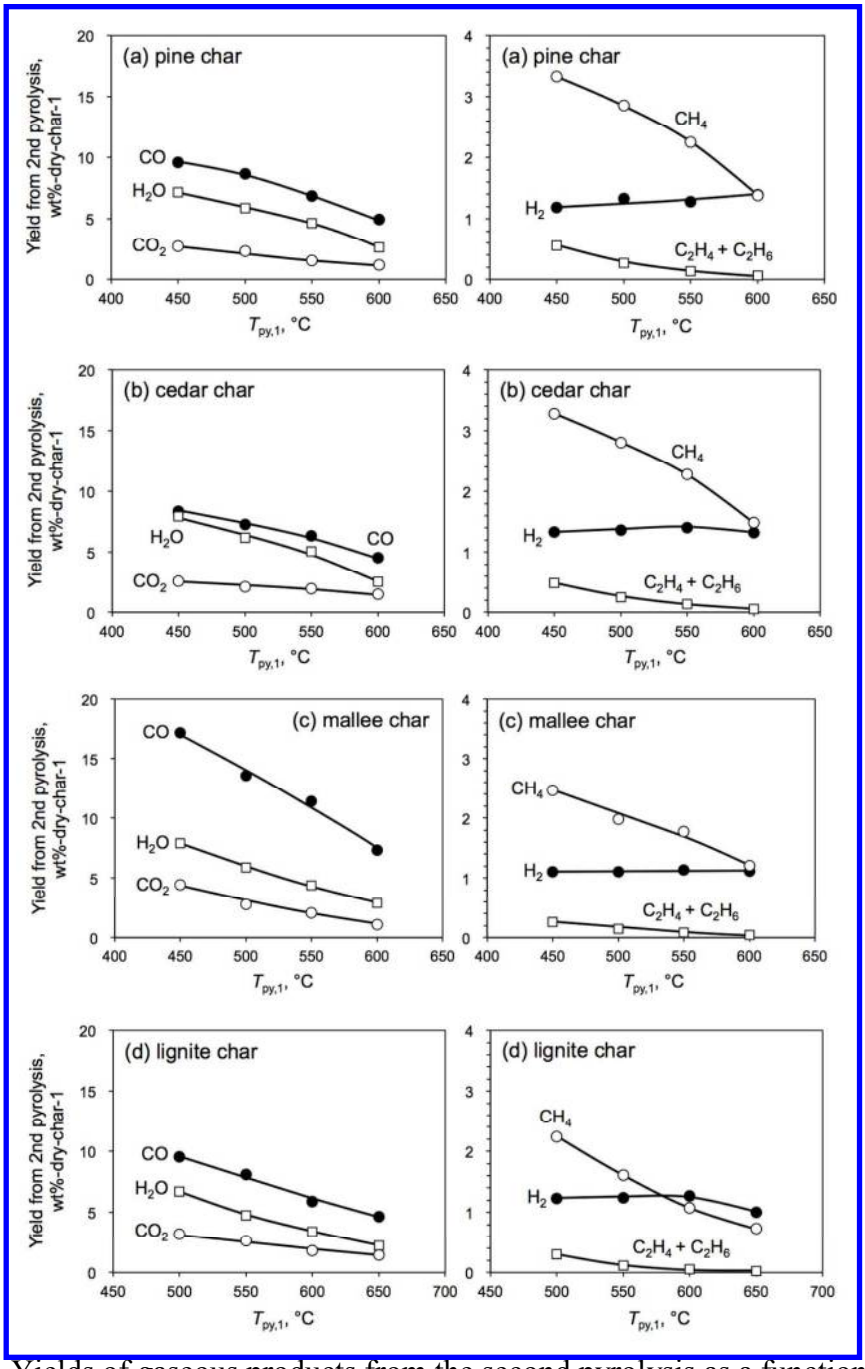

Figure 5. Yields of gaseous products from the second pyrolysis as a function of $T_{py,1}$.

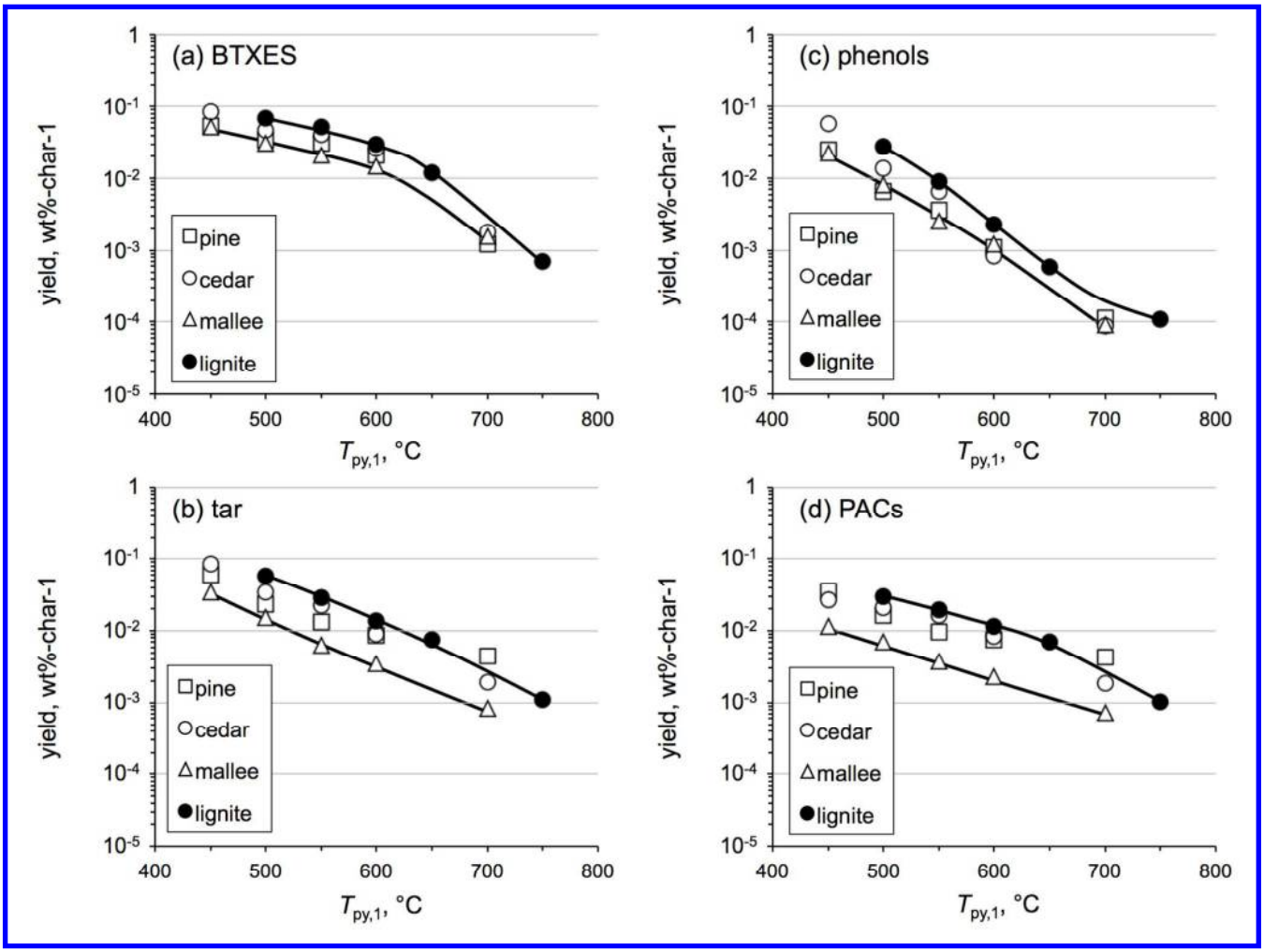

Figure 6. Effects of $T_{py,1}$ on the yields of BTXES (benzene, toluene, xylenes, ethylbenzene and styrene), tar, phenols (phenol, cresols, xylenols, 2-methoxyphenol and 2-methoxy-4-methylphenol) and polyaromatic compounds (indene and aromatic hydrocarbons and oxygenates that have 5–12 double bonds per molecule) from the second pyrolysis.

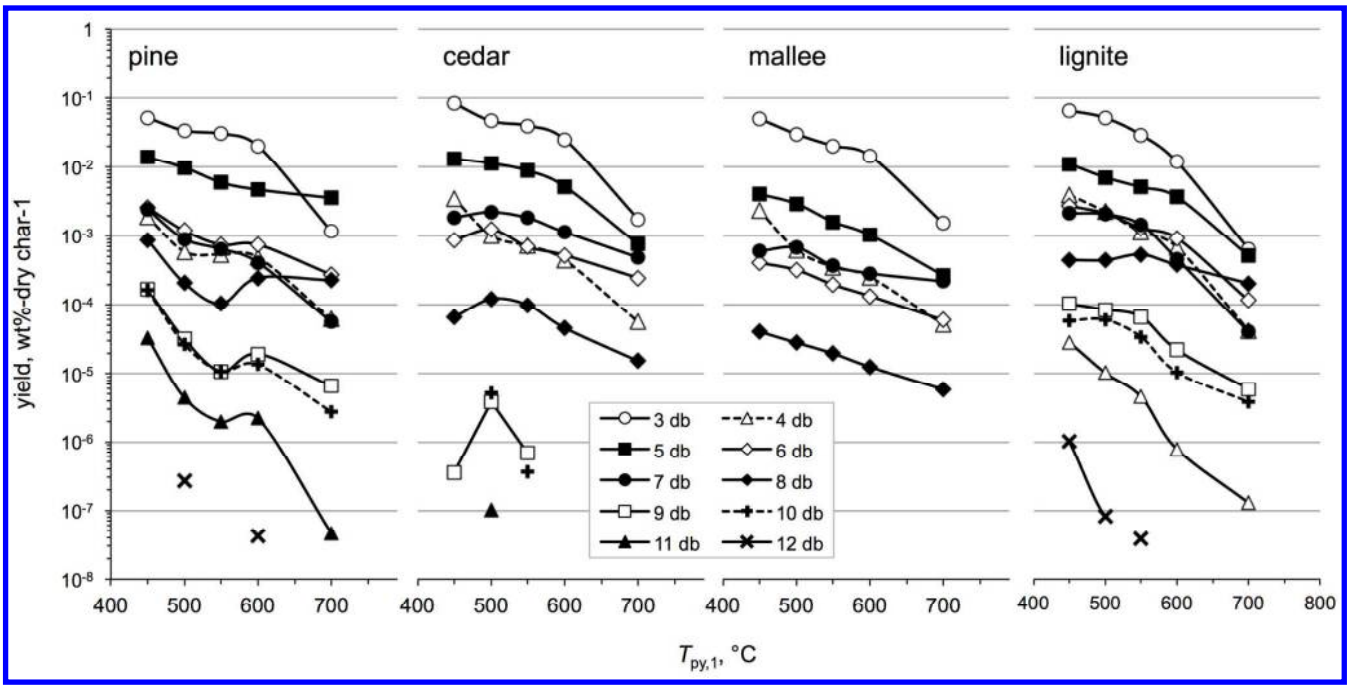

Figure 7. Yields of individual aromatic hydrocarbon homologues from the second pyrolysis of char-1. "db" indicates the number of double bonds per molecule. No oxygen-containing compounds such as phenol, cresols, xylenols, naphthols, benzofuran and dibenzofuran are involved in the homologues.

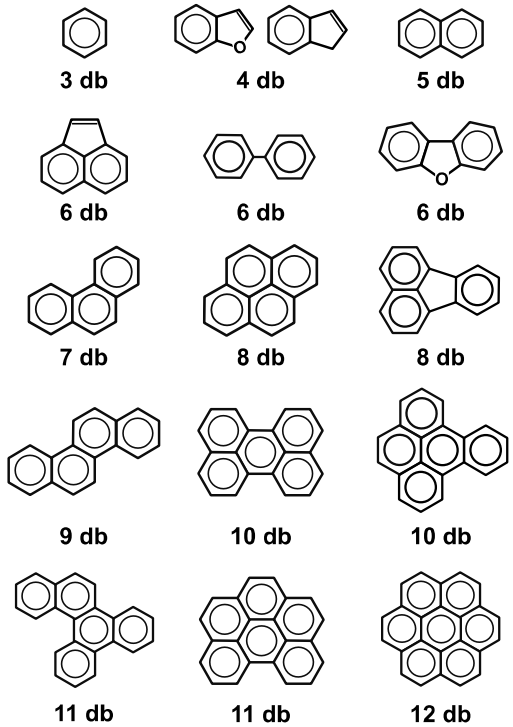

Figure 8. Examples of aromatic compounds with 3–12 double bonds per molecule.

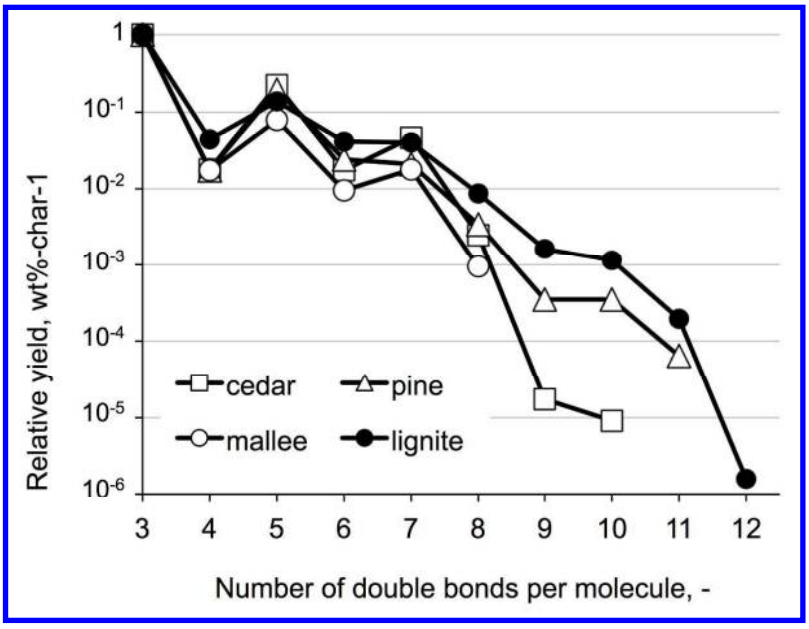

Figure 9. Change in the yield of aromatic hydrocarbon from the second pyrolysis at $T_{py,1}$ = 550 °C as a function of number of double bonds per molecule (d.b.). The yield has been normalized by that of 3 d.b. aromatic hydrocarbon for every char-1.

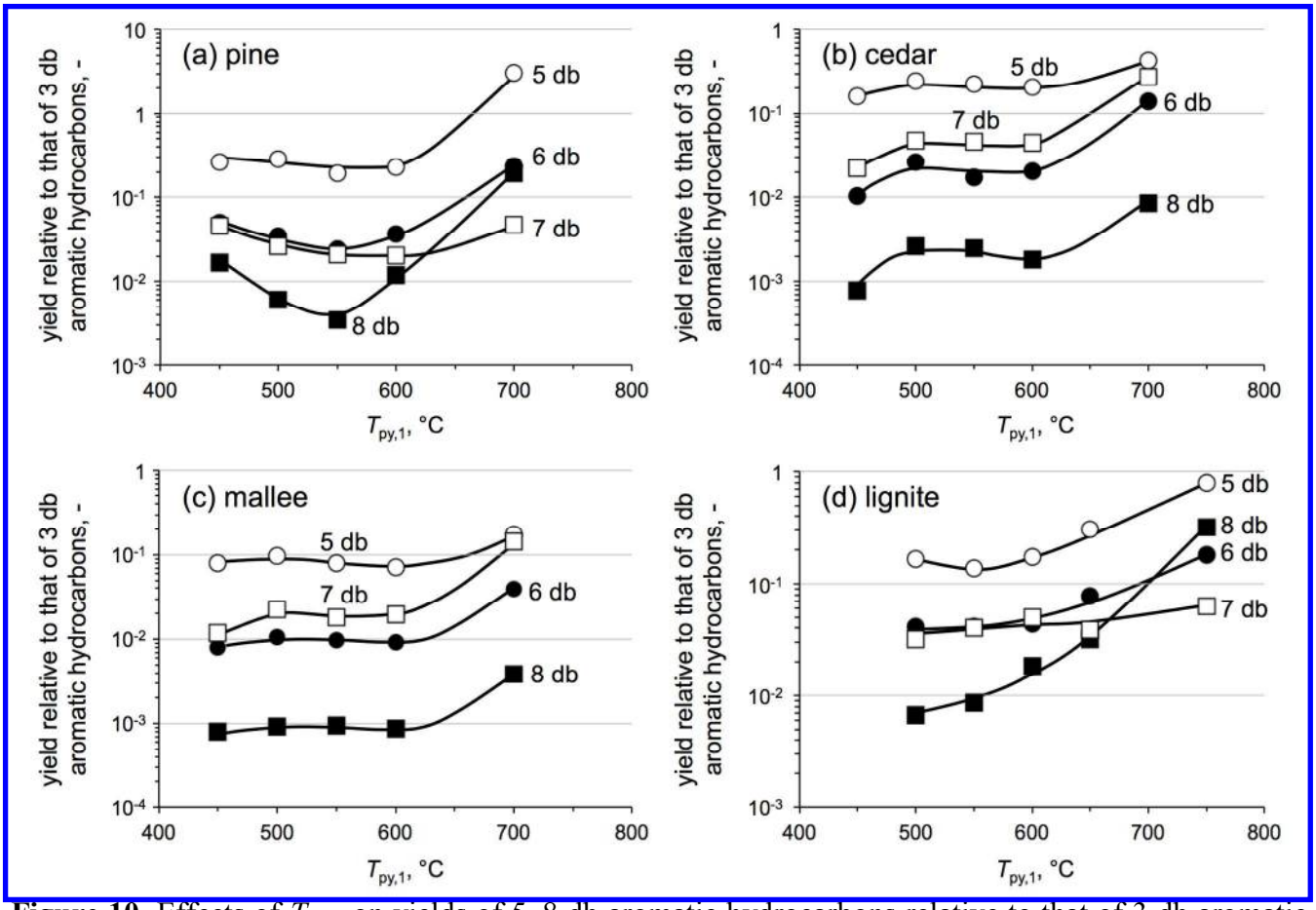

Figure 10. Effects of $T_{py,1}$ on yields of 5–8 db aromatic hydrocarbons relative to that of 3 db aromatic hydrocarbons from the second pyrolysis of char-1.

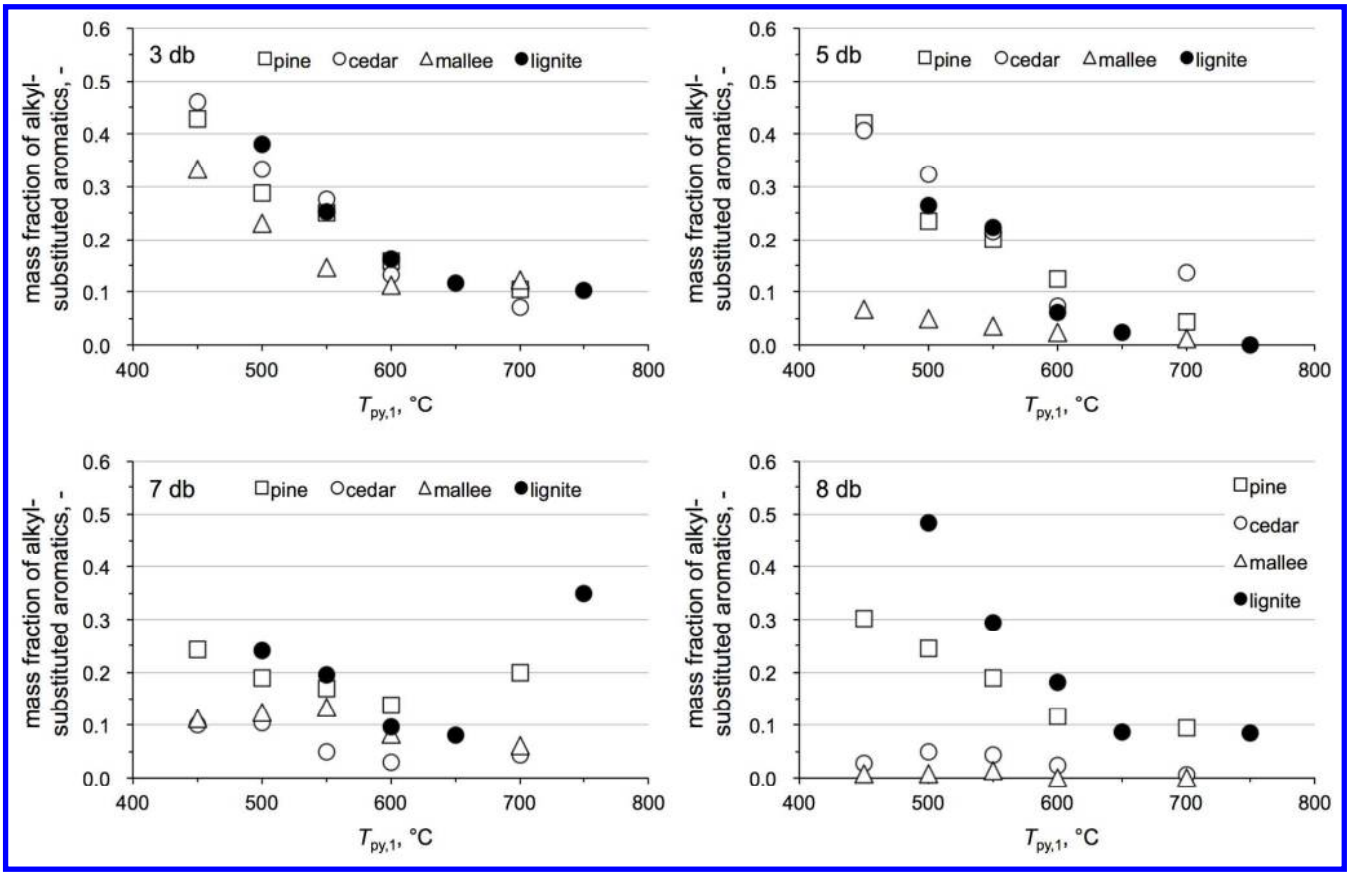

Figure 11. Effects of $T_{py,1}$ on mass fractions of alkyl-substituted aromatic hydrocarbons in 3, 5, 7 and 8 db aromatic hydrocarbons.

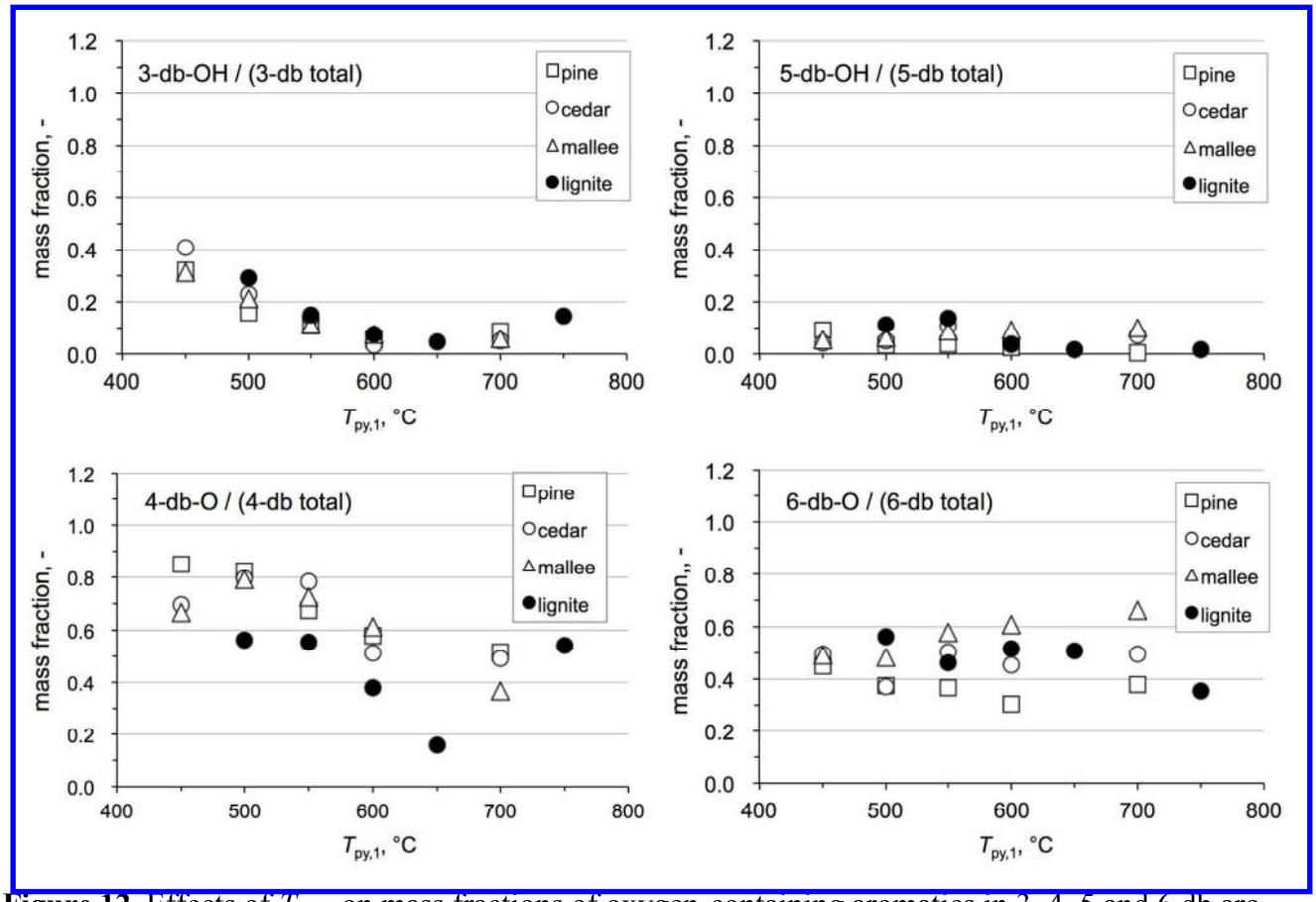

Figure 12. Effects of $T_{py,1}$ on mass fractions of oxygen-containing aromatics in 3, 4, 5 and 6 db aromatic compounds. 3-db-OH; 3 db aromatics with one or two hydroxylic groups, 4-db-O: benzofurans, 5-db-OH; naphthols, 6-db-O; dibenzofurans.